Dalton Transactions

Displacement of ethene from the decamethyltitanocene-ethene complex with internal alkynes, substituent-dependent alkyne-to-allene rearrangement, and the electronic transition relevant to back-bonding interaction.

Journal:	*Dalton Transactions*
Manuscript ID:	DT-ART-01-2015-000351.R1
Article Type:	Paper
Date Submitted by the Author:	25-Feb-2015
Complete List of Authors:	Pinkas, Jiri; J. Heyrovsky Institute of Physical Chemistry, AS CR, Synthesis and Catalysis Gyepes, Róbert; J. Selye University, Faculty of Education Cisarova, Ivana; Charles University, Inorganic Chemistry Kubišta, Jiří; J. Heyrovsky Institute of Physical Chemistry, AS CR, Synthesis and Catalysis Horacek, Michal; J. Heyrovsky Institute of Physical Chemistry, AS CR, Synthesis and Catalysis Mach, Karel; J. Heyrovsky Insitute of Physical Chemistry,

Displacement of ethene from the decamethyltitanocene-ethene complex with internal alkynes, substituent-dependent alkyne-to-allene rearrangement, and the electronic transition relevant to back-bonding interaction

Jiří Pinkas,[a] Róbert Gyepes,[b,c] Ivana Císařová,[c] Jiří Kubišta,[a] Michal Horáček,[a] Karel Mach*[a]

[a] *J. Heyrovský Institute of Physical Chemistry, Academy of Sciences of the Czech Republic, v.v.i., Dolejškova 3, 182 23 Prague 8, Czech Republic.E-mail:karel.mach@jh-inst.cas.cz*

[b] *J. Selye University, Faculty of Education, Bratislavská cesta 3322, 945 01 Komárno, Slovak Republic*

[c] *Department of Inorganic Chemistry, Charles University, Hlavova 2030, 128 40 Prague 2, Czech Republic*

† Dedicated to Volodya V. Burlakov on the occasion of his 60th birthday. Volodya has outstandingly contributed to low-valent early transition metal-alkyne chemistry.

‡ Electronic supplementary information (ESI) available: CIF file for the structures **4**, **6**, **7**, and **11**. Table of crystallographic data and data collection and structure refinement details for **4**, **6**, **7**, and **11**. Electronic absorption spectra for **1**, and **3**–**9**. Atom coordinates for optimized molecules **1**, and **3**–**9**. Projections of MO orbitals Ψ_1, Ψ_2, and Ψ_3 onto the plane containing the titanium and acetylenic carbon atoms. CCDC 1045442 (**3**), 1045443 (**4**), 1045444 (**7**), and 1045445 (**11**). For ESI and crystallographic data in CIF format see …

Received

The titanocene-ethene complex [Ti(II)(η^2-C_2H_4)(η^5-C_5Me_5)$_2$] (**1**) with simple internal alkynes $R^1C{\equiv}CR^2$ gives complexes [Ti(II)(η^2-$R^1C{\equiv}CR^2$)(η^5-C_5Me_5)$_2$] {R^1, R^2: Ph, Ph (**3**), Ph, Me (**4**), Me, $SiMe_3$ (**5**), Ph, $SiMe_3$ (**6**), t-Bu, $SiMe_3$ (**7**), and $SiMe_3$, $SiMe_3$ (**8**). In distinction, alkynes with R^1 = Me and R^2 = *t*-Bu or i-Pr afford allene complexes [Ti(II)(η^2-CH_2=C=CH R^2)(η^5-C_5Me_5)$_2$] (**11**) and (**12**), whereas for R^2 = Et a mixture of alkyne complex (**13A**) with minor allene (**13**) is obtained. Crystal structures of **4**, **6**, **7** and **11** have been determined; the latter structure proved the back-bonding interaction of the allene terminal double bond. Only the synthesis of **8** from **1** was inefficient because the equilibrium constant for the reaction

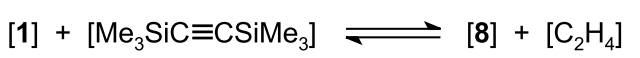

approached 1.

Compound **9** (R^1, R^2: Me), not obtainable from **1**, together with compounds **3–6** and **10** (R^1, R^2: Et) were also prepared by alkyne exchange with **8**, however, this reaction did not take place in attempts to obtain **7**. Compounds **1** and **3–9** display the longest-wavelength electronic absorption band in the range 670–940 nm due to the HOMO→LUMO transition. The assignment of the first excitation to be of predominantly a $b_2 \rightarrow a_1$ transition was confirmed by DFT calculations. The calculated first excitation energies for **3–9** followed the order of hypsochromic shifts of the absorption band relative to **8** that were induced by acetylene substituents: Me > Ph >> $SiMe_3$. Computational results have also affirmed the back-bonding nature in the alkyne-to-metal coordination.

Introduction

The synthesis and crystal structure determination of the title complex [Ti(II)(η^2-C_2H_4)(Cp*)$_2$] (Cp* = η^5-C_5Me_5) (**1**) reported by J. E. Bercaw in 1983[1] confirmed the concept of back-bonding interaction of titanocene(Ti^{II}) with ligands having unsaturated C-C bonds. This concept had already been proposed by Lauher and Hoffmann on the basis of EHMO calculation for the titanocene-ethene complex seven years earlier.[2] Apart from this milestone in understanding organic-metal bonds, Bercaw and Cohen also investigated the reactivity of compound **1** towards a number

of organic reagents, including terminal and internal alkynes, nitriles, acetaldehyde, and carbon dioxide. For the case of internal alkynes, their reaction mode was dependendent on the alkyne substituents used. But-2-yne reacted with **1** via cycloaddition yielding a titanacyclopentene product (**2**), whereas diphenylethyne displaced ethene and formed the titanocene-alkyne complex (**3**) (Scheme 1).[3]

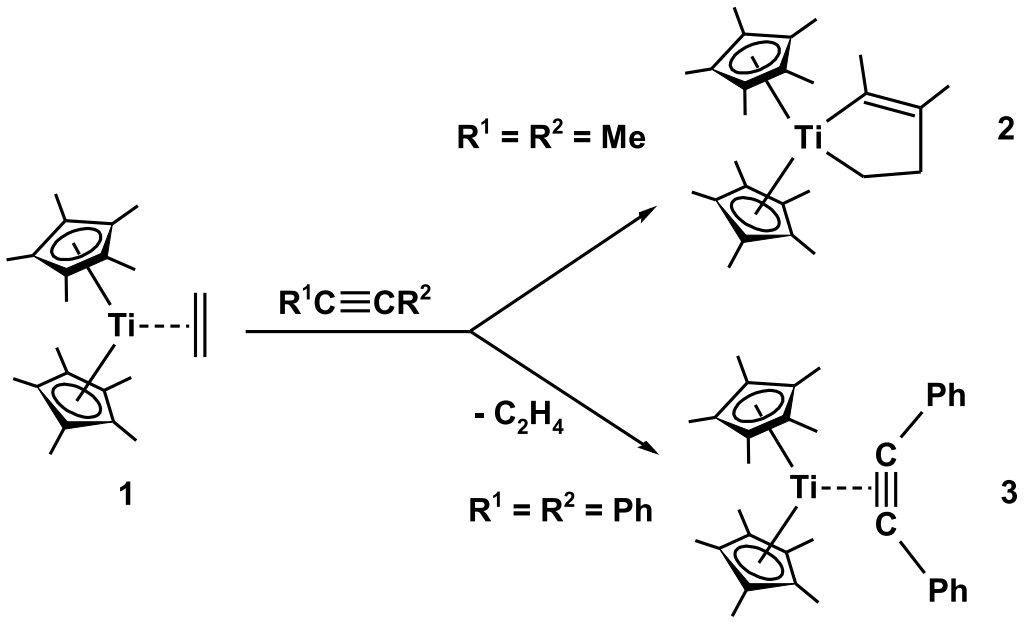

Scheme 1 Different reactivity of **1** towards but-2-yne and diphenylethyne

Recently, compound **1** itself was found to eliminate cleanly ethene upon sublimation under high vacuum providing decamethyltitanocene [Ti(η^5-C_5Me_5)$_2$], whereas heating of **1** in solution to 100 °C resulted in the formation of the doubly tucked-in titanocene accompanied by elimination of ethane (Scheme 2).

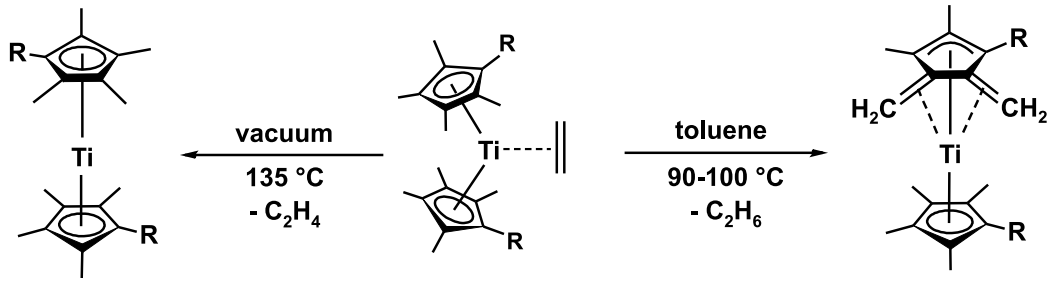

R = Me (**1**), CMe_3, $SiMe_3$

Scheme 2 Thermal elimination of ethene from **1**.

However, the above cycloaddition reaction of but-2-yne with the coordinated ethene (Scheme 1) does not proceed for the titanocene-(η^2-ethene) complexes containing the bulky $SiMe_3$ or CMe_3 groups on otherwise permethylated cyclopentadienyl ligands. Instead, the titanocene-(η^2-MeC≡CMe) complexes are formed (Scheme 3), apparently due to a high steric hindrance in transient complexes precluding the simultaneous coordination of ethene and but-2-yne.[4]

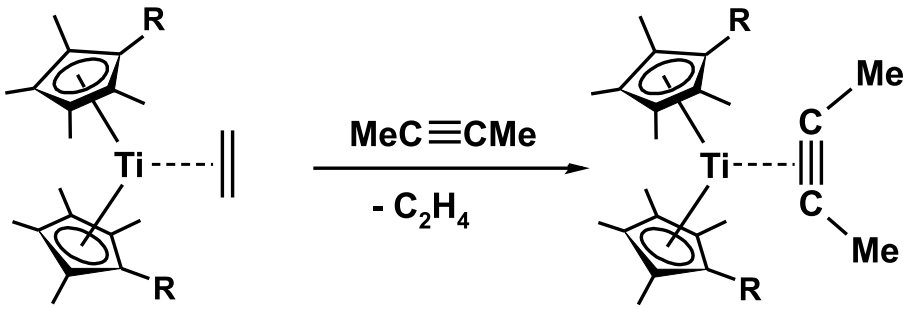

R = CMe_3, $SiMe_3$

Scheme 3 Replacement of ethene with but-2-yne at bulky titanocenes.

Here we report that internal alkynes bearing at least one bulkier substituent than methyl react with **1** exclusively by ethene displacement affording the [Ti(η^5-C_5Me_5)$_2$(η^2-$R^1C{\equiv}CR^2$)] complexes, as reported previously for diphenylethyne (Scheme 1).[1] This method is an alternative to the well-known synthesis of these complexes, which consists of reducing permethyltitanocene dichloride with magnesium in the presence of the respective alkyne in tetrahydrofuran. The latter method has been convenient for alkynes reluctant to undergo addition or cycloaddition reactions, as e.g., bis(trimethylsilyl)acetylene (BTMSA).[5] In particular, titanocene-(η^2-BTMSA) complexes have been widely explored to mimic reactions of titanocenes with a range of reagents, having large impact on the development of titanocene chemistry and its application in organic synthesis.[6] In contrast to the BTMSA case, however, an attempted preparation of analogous (η^2-but-2-yne)

complex by the magnesium-reduction method resulted in the formation of an entirely different Ti(III) product (Scheme 4).[7]

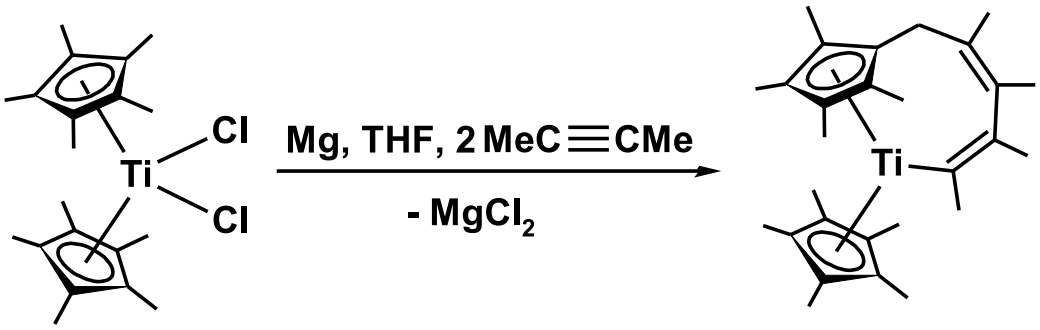

Scheme 4 Formation of a Ti(III) product in the presence of but-2-yne.

For a series of [Ti(η^5-C_5Me_5)$_2$(η^2-$R^1C{\equiv}CR^2$)] complexes obtained, the effects of alkyne substituents (R^1,R^2) on ease of their synthesis, their X-ray crystal structure geometry, chemical shifts in ^{1}H and ^{13}C NMR spectra, ν(C≡C) vibration wavenumbers in infrared spectra, and on the position of their longest wavelength electronic absorption band are investigated. The lowest energy transition for a number of the optimized alkyne complexes and compound **1** were determined by DFT computations and values obtained were compared with experimental data in order to prove the suitability of applied computational methods and bonding model proposed.

Results and discussion

Reaction of 1 with internal alkynes

Compound **1** reacted with internal alkynes $R^1C{\equiv}CR^2$ by ethene replacement as shown in Scheme 5. Only but-2-yne underwent oxidative addition to **1** affording Ti(IV) titanacyclopentene complex **2** as reported previously (Scheme 1).[3,4]

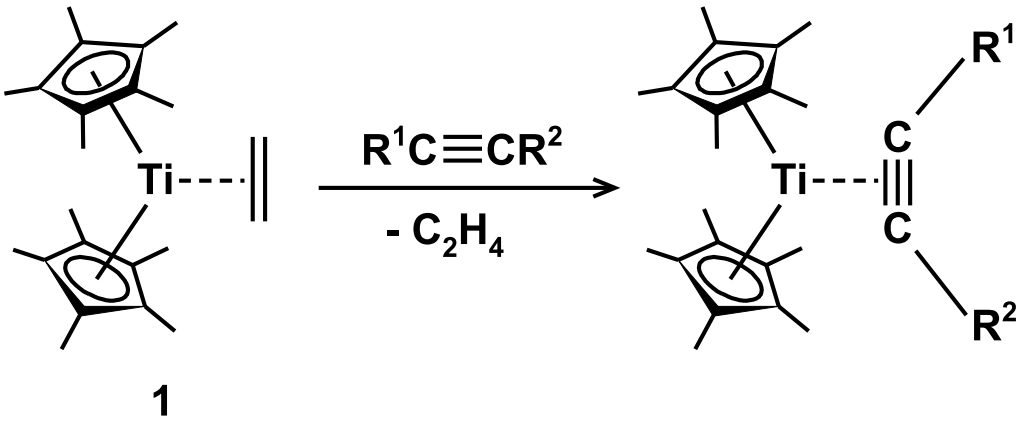

1

R^1	R^2	
Ph	Ph	**3**
Me	Ph	**4**
Me	$SiMe_3$	**5**
Ph	$SiMe_3$	**6**
t-Bu	$SiMe_3$	**7**
$SiMe_3$	$SiMe_3$	**8**

Scheme 5 Reaction of **1** with internal alkynes

The feasibility of ethene replacement depended on the nature of alkyne substituents R^1 and R^2. Complexes containing only carbyl substituents – Ph (**3**) or Ph and Me (**4**) – could be obtained by adding 2 molar equivalents of the alkyne, followed by evaporating all volatiles from the solution after stirring it overnight. However, complexes containing one trimethylsilyl substituent (**5–7**) required heating to 60 °C followed by evaporating all volatiles under vacuum, then introducing another portion of the alkyne and toluene, heating again to 60 °C and finally evaporating all volatiles. An even lower reactivity was observed for BTMSA. The above treatment of **1** with 2 equivalents of BTMSA was repeated three times, and the presence of **1** (1–3 %) in addition to **8** could still be detected by ^{1}H and ^{13}C NMR spectra. The reverse reaction

of ethene added to **8** was followed by ^{1}H NMR spectra in a flame sealed probe. The exchange reaction (1) proceeded at a very slow rate at room temperature.

$$[\mathbf{8}] + [C_2H_4] \underset{}{\overset{K}{\rightleftharpoons}} [\mathbf{1}] + [\mathrm{BTMSA}] \qquad (1)$$

After heating to 60 °C for 8 h and then keeping the sample at room temperature for 2 weeks, the concentrations of all components for reaction (1) were determined by ^{1}H NMR spectra, with an estimate of the reaction equilibrium constant K = 0.9. This value encountered only minor changes after repeated sample heating and measurements in the time scale of six months. A slight uncertainty in determining the equilibrium constant was due to some additional ethene consumption in a dimerization/hydrogen transfer reaction (2) yielding butadiene and ethane.

$$3\ C_2H_4 \rightleftharpoons CH_2{=}CH{-}CH{=}CH_2 + C_2H_6 \qquad (2)$$

This reaction has already been observed by Bercaw[1] to proceed extremely slowly upon aging **1** with ethene in toluene solution with a rate of 1–2 turnovers per year.

A similar reactivity of **1** and **8** following from the value of K offered us the usage of **8** instead of **1** in alkyne exchange reactions. In this way, complex [Ti(II)(η^2-MeC≡CMe)(η^5-C_5Me_5)$_2$] (**9**), which could not be obtained from **1** due to formation of **2** (Scheme 1) was prepared from **8** and but-2-yne in excess. Compound **9** was identified by its ^{1}H and ^{13}C NMR spectra as the sole titanium-containing product even after standing for 2 months at room temperature. Unfortunately, any attempts to obtain crystalline **9** were unsuccessful. This was in accordance with previous observations, that compound **9** prepared from [(Cp*$_2$Ti)$_2$(μ-N_2)] and but-2-yne has been observed to be thermally unstable.[3] For the synthesis of thermally stable **3–7** and **10**, mixtures of **8** with at least two-fold molar excess of the alkyne in toluene-d_8 solution were heated to 80 °C for 7 h. However, the very bulky 1-*tert*-butyl-2-(trimethylsilyl)ethyne did not yield **7** even at 100 °C, whereas at 110 °C the formation of the doubly tucked-in titanocene was already observed.

Properties of 3–8

Compounds **3–8** exhibited some decomposition upon melting in sealed capillaries under nitrogen atmosphere. Their EI-MS spectra gave evidence only of the dissociated alkynes and titanocene [$TiCp^*_2$] *m/z* 318 and their fragment ions, which did not allow to distinguish between the ions generated by electron impact from the complex molecule and from the thermally dissociated species. The easy thermal dissociation of neat [$Ti(II)(\eta^2\text{-}Me_3SiC{\equiv}CSiMe_3)(\eta^5\text{-}C_5Me_4SiMe_3)_2$] is known to proceed at only 90 °C yielding the alkyne and the thermally stable titanocene [$Ti(II)(\eta^5\text{-}C_5Me_4SiMe_3)_2$],[8] however, for complexes **3–8** the dissociation induced by electron impact is to be dominating, as argued for EI-MS spectra of [$Ti(II)(\eta^2\text{-}Me_3SiC{\equiv}CSiMe_3)(\eta^5\text{-}Cp)_2$].[9] Compounds **3–8** were also characterized by ^1H and ^{13}C NMR spectra which showed large down-field shifts for the acetylenic carbon atom resonances and by their infrared spectra displaying the valence vibration of the coordinated triple bond at lower wavenumbers with respect to free alkynes (Table 1). Both these phenomena are generally known for a wide range of transition metal - alkyne complexes indicating various strength of alkyne binding in dependence on effectivity of both donation of alkyne π-electrons to empty metal d orbitals and metal d electrons to empty π*- orbitals.[12] For titanocenes(Ti^{II})-BTMSA complexes, some rather extreme shifts Δδ(C≡C) and Δν(C≡C) have been observed,[6a] which were even pronounced for the more electropositive Zr[6b,c,13a] and Hf metallocene complexes.[13b] A smooth decrease in Lewis acidity of the titanium atom in a series of [$Ti(\eta^5\text{-}C_5H_{5-n}Me_n)_2(\eta^2\text{-}Me_3SiC{\equiv}CSiMe_3)$] ($n$ = 0–5) complexes resulted in low-field shifts of ^1H, ^{13}C and ^{29}Si resonances for the coordinated BTMSA ligand and in the decrease of ν(C≡C) vibration wavenumbers (from 1662 cm^{-1} for n = 0 to 1598 cm^{-1} for n = 5), although with unequal increments per one Me substituent.[10] Inspecting Table 1, it is easily demonstrated that only some rough features of the alkyne substituent effects are recognizable. The infrared method of Δν(C≡C) determination suffers from the unavailability of ν(C≡C) values for free symmetrical dialkyl alkynes; the value of 2240 cm^{-1} used for determination of Δν(C≡C) is apparently a lower limit, doubling the increase of 10 cm^{-1} in ν(C≡C) upon going from PhC≡CPh to MeC≡CPh. The ν(C≡C) values for free alkynes thus follow the electron donation power of substituents Me > Ph >> $SiMe_3$ in agreement with similar studies using other transition metals.[12b,c] The Δν(C≡C) values show with confidence only the lowest contribution of $SiMe_3$ group(s) to the stability of alkyne complexes in accordance with the above reactivity

studies in exchange reactions with **1**. In ^{13}C NMR spectra of free alkynes, the substituents induced chemical shifts changing down-field in the same order. In the titanocene-(η^2-alkyne) complexes even more pronounced substituent effects were observed, having resonances shifted down-field by more than 100 ppm. Rather surprisingly, the $\Delta\delta(C\equiv C)$ values showed the lowest value for compound **3**, whereas the highest value occurred for compound **8**. For the mixed alkyl(aryl)/trimethylsilyl complexes no simple correlation of either $\Delta\delta(C\equiv C)$ or $\Delta\nu(C\equiv C)$ with the nature of substituents could be outlined. The above results rise the question whether subtraction of $\delta(C\equiv C)$ and $\nu(C\equiv C)$ values for complexes from those of free alkynes is justified to determine the strength of the alkyne coordination, since the free and coordinated forms of alkyne are different entities acquiring disparate electronic and geometric structures. The common back-bonding mode of alkyne coordination was proved for **4** and **7** by X-ray single crystal diffraction analysis, however, differences in the Ti–C and C–C bond lengths were within three-fold standard deviations for the structurally characterized complexes **3**, **4**, and **6–8** (see below).

Formation of allene complexes

In contrast to the above alkynes, 1-*tert*-butylpropyne and 1-*iso*-propylpropyne reacted with compound **1** to give the allene complexes **11** and **12** (Scheme 6).

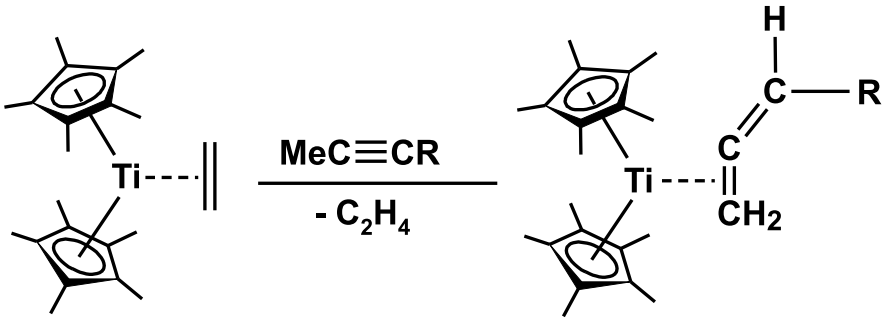

R	yield
t-Bu	**11** (100%)
i-Pr	**12** (~ 85%)
Et	**13** (35%)

Scheme 6 Formation of allene complexes.

The acetylene-to-allene isomerization, induced by coordination to titanium was indicated by ^{1}H and ^{13}C NMR spectra, and its proof for **11** was provided by its crystal structure (see below). The ^{1}H NMR spectrum of allene moiety displayed the AB_2 system for C*H* and CH_2 groups with the coupling constant $^{4}J_{HH}$ about twice smaller than that for the free allene CH_2=C=CH(*t*-Bu). The ^{13}C resonances of the coordinated double bond were shifted down-field with respect to those for the free allene CH_2=C=CH(t-Bu) (Table 2),[14] with δ(*C*H_2=) occuring between the value for coordinated ethene in **1** (105.1 ppm)[1] and that for the exomethylene groups in the doubly tucked-in titanocene [Ti(C_5Me_5)(C_5Me_3(CH_2)$_2$}] (67.6 ppm).[15] Compound **12** could not be purified by crystallisation, however, ^{1}H and ^{13}C NMR spectra of the main product (85%) were similar in all respects to those of **11**, indicating an analogous coordination of the allene CH_2=C=CH($CHMe_2$). The presence of titanocene-alkyne complex was not observed among the byproducts of **12**, however, the reaction of **1** with pent-2-yne afforded an equilibrium of a less abundant allene complex [Ti(C_5Me_5)$_2$(η^2-CH_2=C=CHEt)] (**13**) and an overwhelming alkyne complex [Ti(C_5Me_5)$_2$(η^2-MeC≡CEt)] (**13A**) in a crude reaction product. The above assignment for the allene complexes is corroborated by agreement with ^{1}H and ^{13}C NMR spectra for the phenylallene complex [Ti(C_5Me_5)$_2$(CH_2=C=CHPh)] (**14**) which, although unassigned for the lack of structural information,[16] agree closely with the data for **11**–**13** (Table 2).

Table 2 NMR data for allene moieties in **11**–**13** and allene CH_2=C=CH(t-Bu) (**A**)

Cpd.	C*H*	CH_2	$^{4}J_{HH}$ [Hz]	=*C*H_2	=*C*H	=*C*=	Ref.
11	3.50	2.03	3.3	84.66	128.30	231.20	This work
12	3.64	2.17	2.4	86.38	127.48	234.56	This work
13	2.79-3.90	2.16-2.22	Not available	86.90	121.90	237.05	This work

14	5.12	2.60	3.3	86.54	120.83	244.15	16
A[a]	5.09	4.69	6.8	76.3	101.9	205.7	14

[a] Measured in $CDCl_3$.

The other known titanocene-allene complexes were obtained by reacting allenes with one molar equivalent of $[Ti(C_5H_5)_2(PMe_3)_2]$ or $[Ti(C_5H_5)_2(PMe_3)(C_2H_4)]$. The crystal structure of $[Ti(C_5H_5)_2(PMe_3)(CH_2{=}C{=}CPh_2)]$ shows the coordination of the $CH_2{=}C$ bond and ^1H and ^{13}C NMR data are compatible with those presented in Table 2.[17] A thorough ^1H NMR monitoring of isomerisation of η^3-allyl to (E)-1-propenyl at the singly tucked-in titanocene by G.A. Luinstra et al.[18] allowed to establish the reaction pathway involving the intermediate formation of titanocene-η^2-allene, which isomerized further providing titanocene-η^2-propyne in the penultimate step. The reverse isomerisation of coordinated alkynes to allenes in the present case is apparently induced by a larger electron donating ability and/or steric bulkiness of *tert*-butyl and *iso*-propyl substituents which is also expressed in yields of **11–13** (Scheme 6). The necessary C^1–C^3 hydrogen shift is apparently initiated by agostic interaction[19] of one hydrogen atom of the methyl group to the metal followed by its abstraction in an oxidative addition step (Ti^{II} – Ti^{IV}). The hydrogen transfer in titanium coordination sphere to C^3 accompanied with rearrangement to allene accomplishes the reductive elimination step as depicted in Scheme 7.

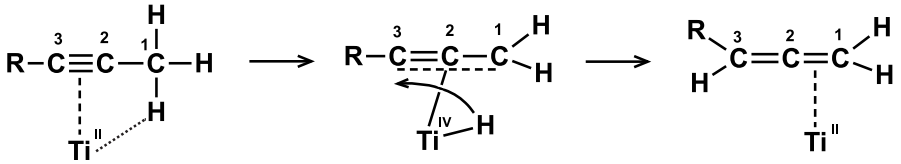

Scheme 7 Proposed steps in η^2-alkyne – η^2-allene rearrangements.

A strong base-induced isomerization of internal alkynes to allenes is commonly known,[20a] and transition metals are known to participate in such isomerizations.[20b] The alkyne-to-allene isomerization within the defined transition metal complexes are rather scarce, and in some cases require acido-basic promotion.[21]

The thermally induced isomerizations on Re,[22a] Os,[22b] and Ir[22c] are generally much slower than the present one that occurs immediately after addition of the 1-alkylpropynes to **1** at room temperature.

Reactions of 1 with conjugated diynes and enynes

Compound **1** reacted smoothly with one molar equivalent of 1,4-bis(trimethylsilyl)buta-1,3-diyne, 1,4-diphenylbuta-1,3-diyne, and 2,2,7,7-tetramethylocta-3,5-diyne to give nearly quantitatively the known products **15**, **16**, and **17**, respectively (Scheme 8) . All have been obtained by U. Rosenthal et al. upon reducing $[Ti(C_5Me_5)_2Cl_2)]$ with one equivalent of magnesium in the presence of the diynes; however, they could not be obtained by the ligand replacement from compound **8**.[23a,b]

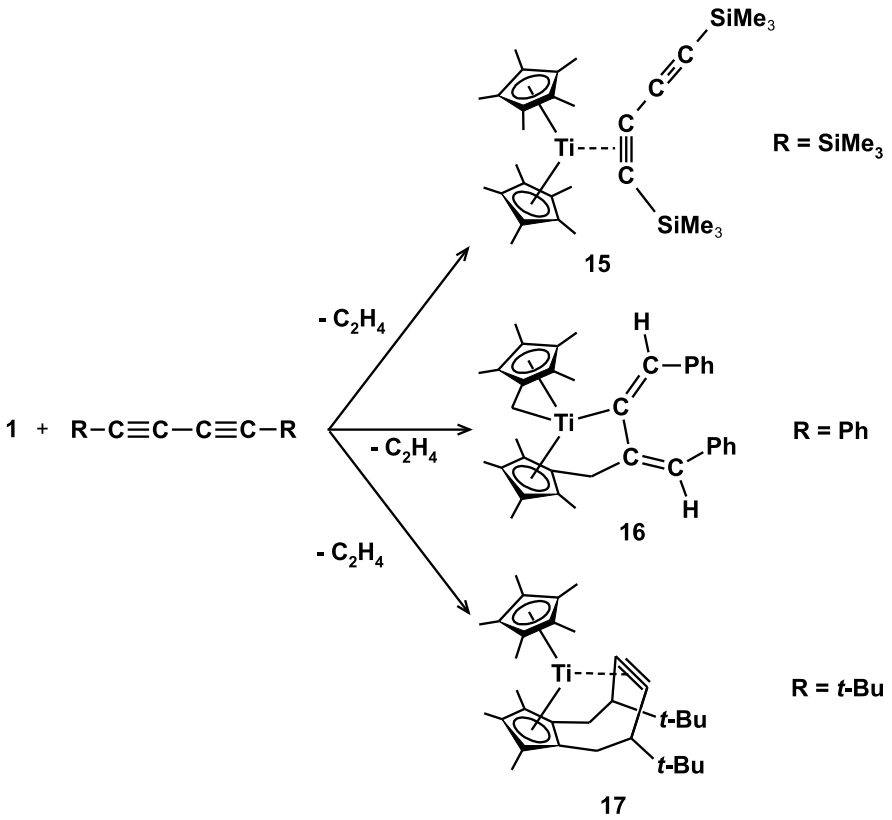

Scheme 8 Reaction of **1** with 1,4-substituted buta-1,3-diynes.

The present results prove that the unexpected complex rearrangements, leading to the formation of **16** and **17** are induced only by replacing the ethene in **1** for the diynes, calling for no involvement of the magnesium. As shown above, the affinity of both BTMSA and ethene to titanocene is similar, so the reported reluctance of complex **8** to react with the former two diynes[23a] indicates that the bulkiness of BTMSA is hindering its displacement.

However, compound **1** also showed a limit in its reactivity upon attempts to react it with head-to-tail dimers of (trimethylsilyl)ethyne and *tert*-butylethyne. While eager to react with 2,4-bis(trimethylsilyl)but-1-ene-3-yne to give product **18** (Scheme 9), obtained previously by the reduction of $[TiCp^*_2Cl_2]$ with Mg in the presence of the dimer,[23c] compound **1** remained intact even after warming with 2,4-di-*tert*-butylbut-1-ene-3-yne to 60 °C for 18 h.

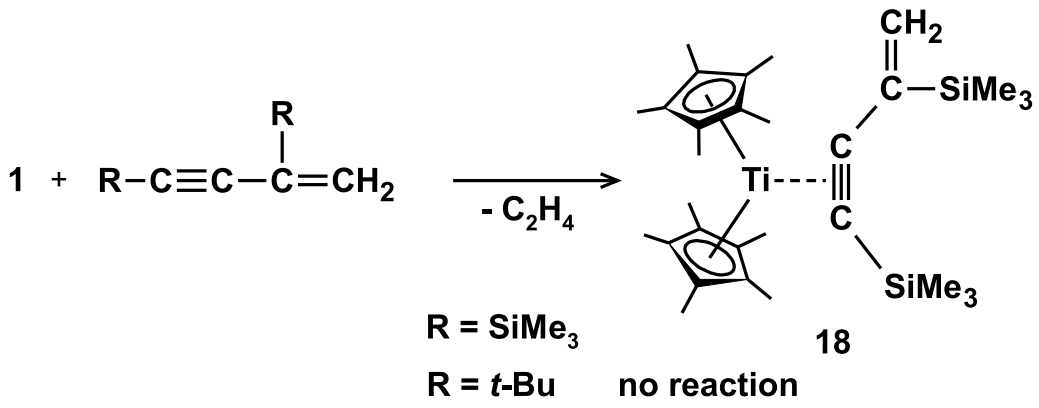

Scheme 9 Reaction of **1** with 2,4-disubstituted but-1-ene-3-ynes.

Since the latter dimer, (trimethylsilyl)*t*-butylethyne and BTMSA did not react with the singly tucked-in titanocene $[Ti(C_5Me_5)(C_5Me_4(CH_2)\}]$ even after warming to 80 °C for 3 days,[7b] the formation of compounds **7** and **8** presented in this work points to a superior reactivity of **1**.

Crystal structures of 4, 6, 7, and 11.

PLATON drawings for **4** and **7** are shown in Fig. 1 and Fig. 2, respectively, and important geometric parameters for compounds **4**, **6**, and **7** are listed in Table 3.

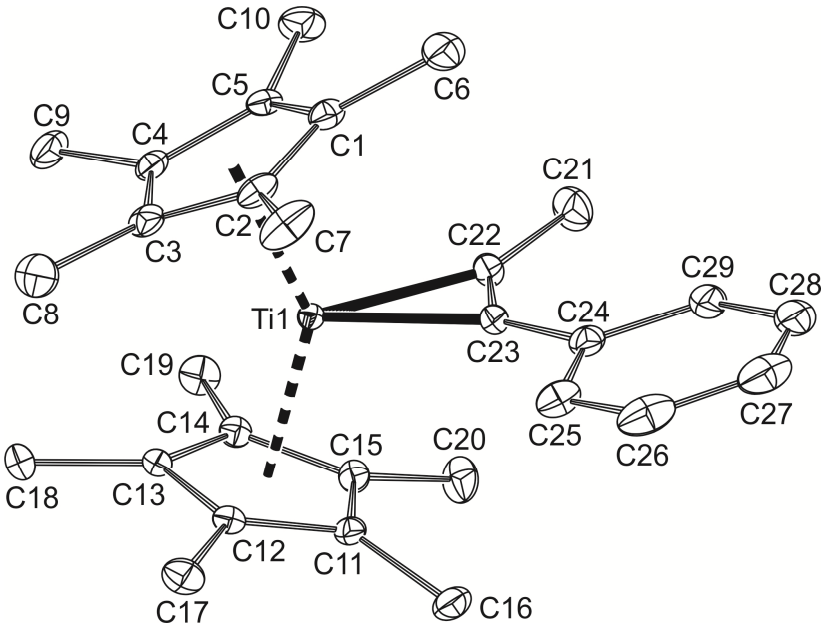

Fig. 1 PLATON drawing of **4** at the 30% probability level, including the atom labeling scheme. Hydrogen atoms are omitted for clarity.

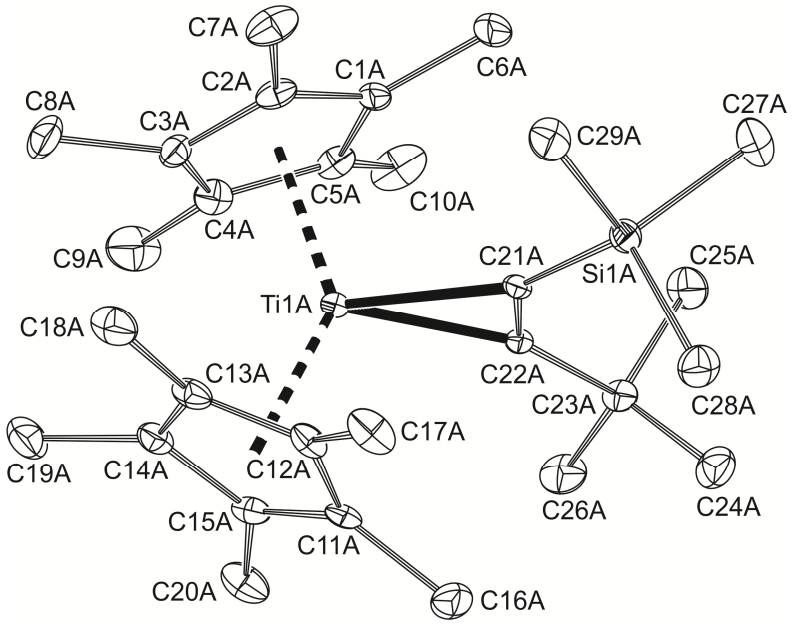

Fig. 2 PLATON drawing of molecule 1 of **7** at 30% probability level, including the atom labeling scheme. Hydrogen atoms are omitted for clarity.

Our efforts to obtain compound **6** in crystalline form resulted in an orthorhombic polymorph, which afforded slightly more precise geometric data than those reported for **6** in a triclinic unit cell (given in parentheses).[11b] In attempts to recognize effects of the alkyne substituents on the strength of back-bonded alkyne ligands, relevant data for the previously reported compounds **3**[11a] and **8**[11b] have also been included in Table 3. The most important parameter in this respect is the coordinated triple bond length, since its elongation is directly proportional to the extent of back-bonding to the metal. In complexes of early transition metals, the magnitude of the C≡C bond length elongation may lead to interatomic distances even approaching values appropriate for a bonding order lower by one.[6] For the present complexes, the C(a)−C(b) bond length falls into a narrow interval of 1.296(3)−1.309(4) Å, coming close to a typical C=C (double bond) length (~1.33 Å).[24] Differences in bond lengths are less than three times standard deviations which precludes to establish the influence of the alkyne substituents. For complexes **6** and **7** having asymmetrically substituted alkynes, however, a tiny difference in the Ti−C(a) and Ti−C(b) distances may indicate that carbyl substituents induce slightly stronger Ti−C bonds than the trimethylsilyl one. The bending of alkyne substituents from linear arrangement (angles E(1)−C(a)−C(b) and E(2)−C(b)−C(a)) is nearly independent of the substituent nature, and differences in these angles for different substituents E(1), E(2) are in the range of differences found for **8** with both $SiMe_3$ substituents. The lowest dihedral angle of cyclopentadienyl ring planes (φ) for **4** is compatible with the expected lowest steric congestion between alkyne substituents and cyclopentadienyl ligands. This steric congestion is apparently responsible for the asymmetrically coordinated BTMSA ligand found in **8**. It can be concluded that the solid state structures of decamethyltitanocene-alkyne complexes do not differ sufficiently to reveal the effects of alkyne substituents.

The crystal structure of **11** (Fig. 3) provided evidence for decamethyltitanocene binding the allene ligand via a η^2-coordinated terminal double bond which is considerably elongated with respect to that in non-coordinated allene (av. 1.307 Å).[24]

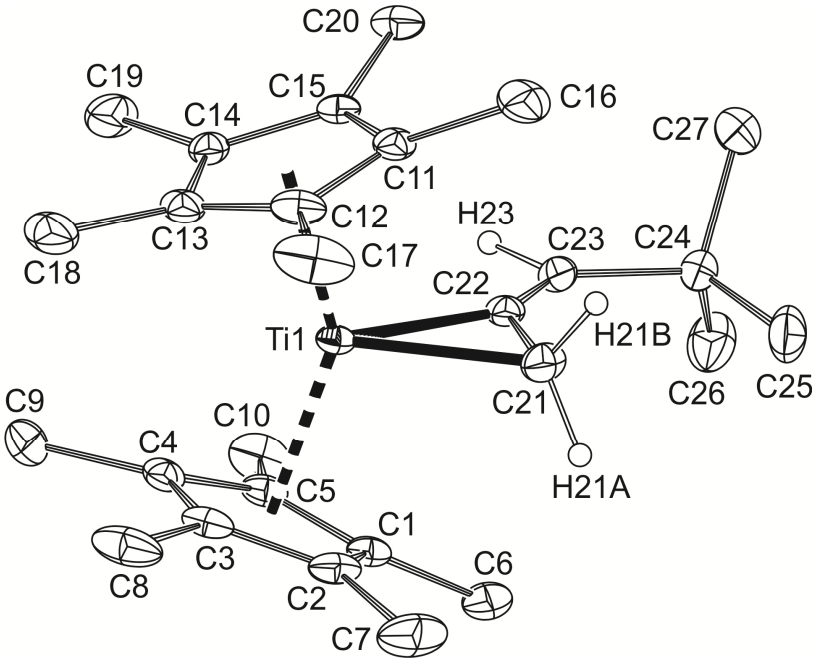

Fig. 3 PLATON drawing of **11** at the 30% probability level, including the atom labeling scheme. Hydrogen atoms are omitted for clarity.

Whereas the vicinal double bond remains virtually unchanged the coordinated double bond is elongated more than that in **1** (1.457(3) Å against 1.438(5) Å[1]). The coordinated double bond is more tightly bound by the central allene carbon atom C(22), exhibiting a shorter Ti–C distance than the methylene carbon atom C(21) (Table 4). Despite this asymmetry, the titanocene plane Cg(1), Ti, Cg(2) nearly exactly bisects the coordinated double bond. The decreased bond order of the coordinated double bond is reflected also in the H(21A)–C(21)–H(21B) angle of 108.6(19)°, approaching the value typical for carbon sp^3 hybridization. The plane of this angle is declined from the C(21)–C(22) line by 34.9° away from titanium, similarly as found for the coordinated ethene in **1**.[1] The allene ligand is bent at C(22), and is nearly perfectly planar around the non-coordinated double bond. The hydrogen atom H(23) is slightly inclined towards the titanium atom, however, the Ti...H(23) distance of 3.48(3) Å is well beyond any effective bonding interaction.[19] The bulky *t*-butyl group is directed away from the open side of the titanocene shell, and its short contact distances to the Cp* ligands exceed those between the Cp* rings. In distinction, the methylene protons H(21A) and H(21B) exert short contact distances to the Cp* carbon atoms (H(21A)...C(6) 2.67(2) Å and H(21B)...C(16) 2.39(3) Å), explaining the reason for large deviations of these methyl carbon atoms from the

least-squares planes of the cyclopentadienyl ligands: C(6) 0.1858(38) Å and C(16) 0.2469(40) Å. This steric congestion is consistent with a longer Ti–C(21) bond compared to Ti–C(22). The only comparable titanocene-allene structure of $[Ti(C_5H_5)_2(PMe_3)(CH_2=C=CPh_2)]$ showed an analogous planar structure around the non-coordinated double bond.[17] A shorter coordinated double bond (1.423(5) Å) and longer Ti–C bonds (2.241(3) Å to $H_2C=$ and 2.188(3) Å to =C=) compared to those of **11** indicate a weaker allene coordination. In zirconocene-cyclic allene (3-methyl-1,2-cyclohexadiene and 3-methyl-1,2-heptadiene) complexes $[Zr(C_5H_5)_2(PMe_3)(-CH=C=CMe(CH_2)_n-)]$ (n = 3 or 4) the Zr–C bond to internal allene carbon atom was also found to be shorter (by more than 0.1 Å) than that to the –CH= carbon atom.[25]

Electronic absorption spectra and computational treatment

Electronic absorption bands for compounds **1** and **3–9** measured in the range 300–1600 nm, coupled with the three lowest excitation energies computed by time-dependent DFT level of theory for the optimized molecules are listed in Table 5. Of particular interest is the position (λ_{max}) of the longest wavelength absorption band, since it exhibits remarkable shifts in connection with the nature of the acetylene substituents – e.g., 670 nm for **9** (Me), 710 nm for **3** (Ph), and 920 nm for **8** ($SiMe_3$) (all spectra of Table 5 are reproduced in the ESI). The computed first excitation energies followed well the sequence of experimental λ_{max} for all acetylene complexes. To find the reason why various substituents exert a different shift in first excitation energies, several quantities have been evaluated and compared (Table 5). However, the only quantity, which exhibited an unequivocal correlation with first excitation energies were Counterpoise energies computed between the bent titanocene moieties and the bent alkyne ligand. Among structural parameters, the optimized Ti–C bond lengths correlated reasonably with computed first excitation energies, which indicated also the dependence upon the strength of alkynes coordination (Fig. 4).

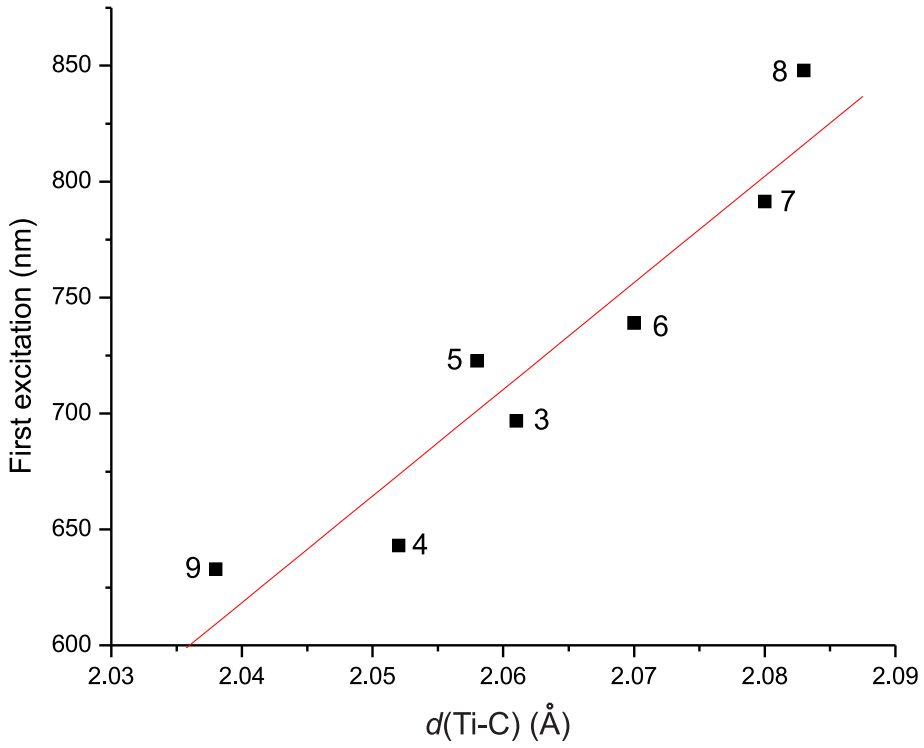

Fig. 4 Correlation between computed first excitation energies and optimized average Ti–C interatomic distance for **3**–**9**.

When optimized acetylenic C–C bond lengths and Mayer bond orders have been correlated with the first excitation energy, neither of these quantities exhibited substantial differences within the series of acetylenic complexes. Only NBO charges of the mentioned atoms q(Ti, C, C) and the resulting charge difference $\Delta q(q(\mathrm{Ti}) - q_{\mathrm{av}}(\mathrm{C}))$ showed a remarkable increase upon the presence of the acetylene $SiMe_3$ substituent(s) reflecting the different nature of the $SiMe_3$. The silicon atom which is more electropositive than carbon atom induces a larger negative charge on acetylenic carbon atoms and increases the ionic contribution to the ligand-metal interaction. For **8** Natural Resonance Theory determined as much as 44.6% of ionic bonding contribution, which underlines the importance of both ionic and covalent contributions to the acetylene coordination.

A good agreement of experimental λ_{max} with computed first excitation energies suggests the applicability of our theoretical model. A more detailed analysis of the final wavefunctions has confirmed the appropriateness of the back-donation model for all of the titanocene-acetylene complexes described above. Canonical molecular obitals (MO's) revealed the coordination of the acetylenic ligands to be achieved through the simultaneous interaction of three atomic centers, generating an interaction resembling a three-center-four-electron (*3c-4e*) bond. This is in complete agreement with requirements imposed by group theory, which requires the two carbon atoms of the acetylenic ligand to act upon coordination as a whole unit, having the same contributions (either bonding or antibonding) from both carbon atoms in every orbital.

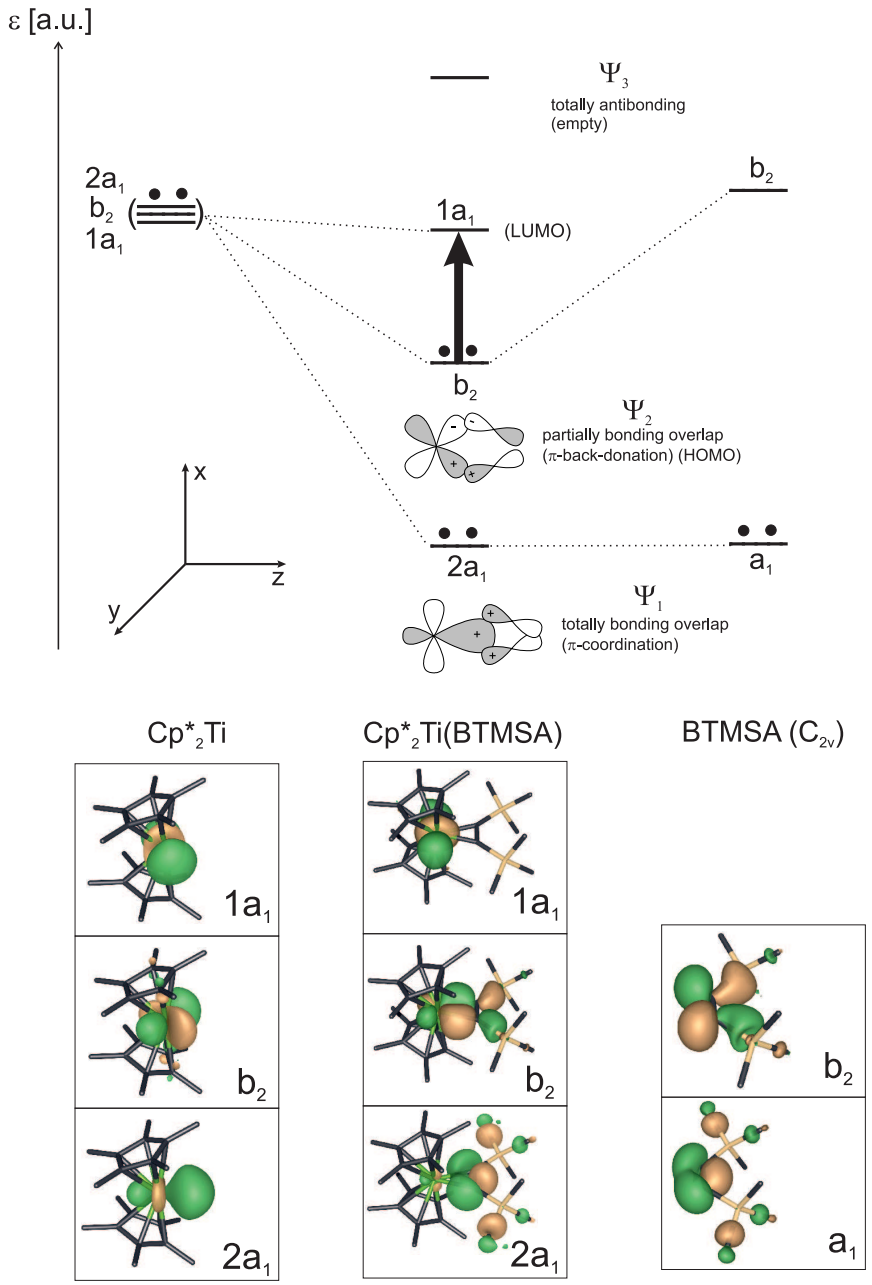

Fig. 5 Interaction diagram of **8**. The Counterpoise computation of the Cp^*_2Ti fragment included also the basis functions of BTMSA and vice versa. The notation of the near-degenerate Cp^*_2Ti orbitals is given in accordance with Lauher and Hoffmann[2] using symmetry labels of point group C_{2v}.

The three-center metal-ligand interaction generates two attractive interactions in alkyne complexes: i) metal–acetylene and ii) overlap between the carbon atoms of the acetylenic ligand (Fig. 5). The totally bonding orbital (Ψ_1) is the σ-donation from the ligand, occurring from the ligand π system to the $2a_1$ of the bent titanocene, although their overlap is very small due to the large energy difference between the two fragment orbitals involved. The next combination is a partially antibonding orbital (Ψ_2), generated by the overlap of the bent titanocene b_2 and the acetylenic π^* orbitals. According to Counterpoise results, both electrons in Ψ_2 are obtained from the bent titanocene, since the corresponding molecular orbital of the acetylenic fragment becomes empty upon separating the bent titanocene and the acetylene fragments to infinite distance. Since Ψ_2 includes both bonding and antibonding contributions (resulting from the population of π^* orbitals), it becomes the molecular HOMO due to its relatively high orbital energy.

The first electronic excitation observed for alkyne complexes is approximately a neat HOMO→LUMO transition. The low energy of this transition, occurring for some complexes even in the near-IR region is the consequence of the rather high energy of the HOMO. The LUMO orbital is the practically unaltered $1a_1$ of the bent titanocene fragment. Even after the alkyne coordination, its perpendicular orientation to the open side of the titanocene shell prevents any major overlapping with either of the ligands. Projections of MO orbitals Ψ_1, Ψ_2, and Ψ_3 onto the plane containing the titanium and acetylenic carbon atoms are depicted in the ESI.

Compounds with effective transition metal-to-alkyne backbonding are commonly called metallacyclopropenes because of their geometry resembling cyclopropene features. A review on bonding in these compounds assumed that the Dewar, Chatt and Duncanson model for bonding of alkenes[26] is to be extended for an interaction of the alkyne orthogonal π-orbital with available metal d-orbital, considering the alkyne to be a four-electron donor.[27] Bonding in early transition (Ti, Zr and Hf) metallocene-BTMSA complexes has been recently investigated by DFT methods. The study concluded that $Ti^{IV}(d^0)$ binds the bent acetylene by two Ti–C σ-bonds and by out-of-plane π-bonding which represents a three-center two-electron (3c-2e) bonding interaction.[28]

Our model for titanocene-alkyne complexes does not reveal any significant bonding interaction between the metal and orthogonal π-orbital of the alkyne (out-of-plane) since the suitable $d_{x,z}$ orbital is largely involved in binding the cyclopentadienyl

ligands. The alkyne can be thus formally considered a two-electron donor, in full agreement with experimental as well as computed bond lengths. The authentic four-electron donor BTMSA ligand was found in [{(COT)Ti}$_2$(η^2: η^2-BTMSA)] (COT = [η^8-C_8H_8]$^{2-}$) complex containing two titanium atoms coordinated perpendicularly to the alkyne triple bond (Chart 1). The C–C bond length of such coordinated alkyne approached the single bond length (av. 1.51 Å).[29] The presence of Ti(II) in **8** was independently proved by the transfer of single electron in the reaction of **8** with 2,2'-bipyridine under formation of electronic triplet state between Ti(III) d-electron and bipyridine radical anion. Analogous reaction of **8** with 4,5-diazafluorene was accompanied by hydrogen elimination yielding Ti(III) – diaza-coordinated fluorenyl compound (Scheme 10).[30]

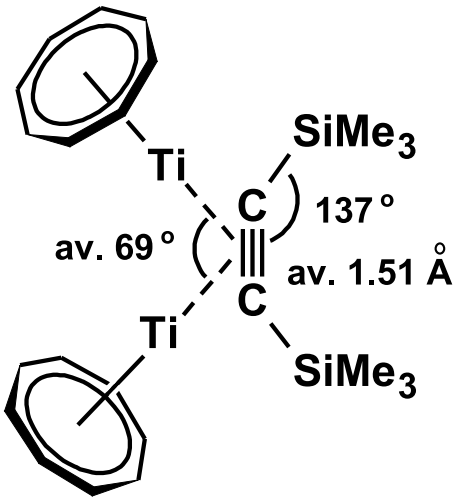

Chart 1 Depiction of [{(COT)Ti}$_2$(η^2: η^2-BTMSA)].[29]

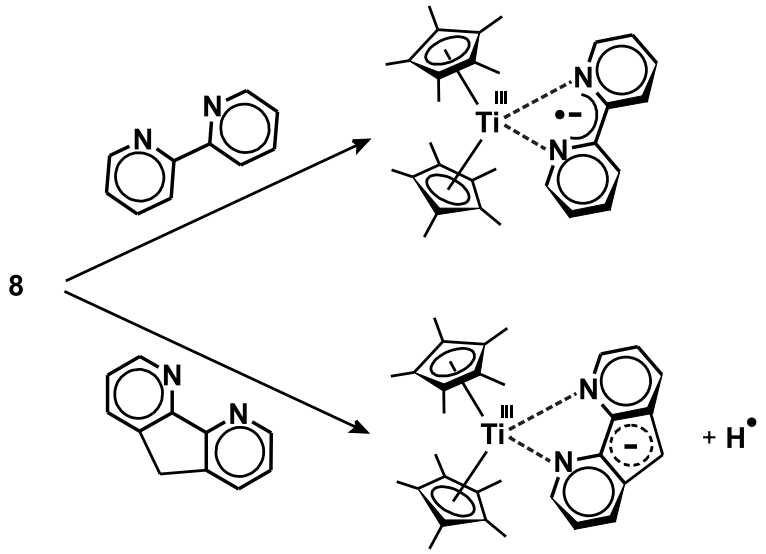

Scheme 10 Single electron transfer reactions of compound **8** with 2,2'-bipyridine and 4,5-diazafluorene.[30]

The presence of Ti(II) in complexes **1**–**9** is in accordance with the relatively high energy of the HOMO causing the HOMO-LUMO transition to occur in near-infrared region for **8**. Bent titanocene (Ti^{IV}) complexes carrying two Ti–C σ-bonds actually incorporate a different combination of titanocene orbitals for the coordination of their σ-donors — one canonical orbital utilizing the $1a_1$, the other the b_2 titanocene MO. Unlike their Ti(II) analogues, Ti(IV) complexes are void of large antibonding contribution to their HOMO; their HOMO energies will thus become lower, inducing a noticeable hypsochromic shift of any potential HOMO→LUMO excitations. As examples, $Cp^*_2TiMe_2$ shows the longest wavelength absorption band at λ_{max} 423 nm[31] and cyclopentadienyl-tethered titanacyclopentanes in the range 560–640 nm.[32] On the other hand, the occurrence of an absorption band in near infrared region (920–1055 nm) for compound **1**, $[(Ti(\eta^5\text{-}C_5Me_4SiMe_3)_2(\eta^2\text{-}C_2H_4)]$[8] and a number of complexes containing the double bond either singly[33a] or doubly tethered to one or two permethylated cyclopentadienyl ligands[33b-d] can be considered indicative of the presence of metal-olefin back-bonding.

Conclusions

Decamethyltitanocene-ethene complex **1** is a suitable reagent for synthesis of internal acetylene complexes **3–8** bearing at least one alkyl or aryl group and one trimethylsilyl group via the ligand exchange reaction (3),

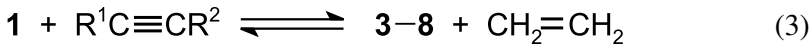

(3)

However, the equilibrium constant of this reaction for **8** approaches 1 (1.16) showing that the easily obtainable reagent **8** can be also used for exchange reactions with other alkynes. In this way, compound **9**, which is otherwise inaccessible via the reaction of but-2-yne with **1**, could be obtained by reacting but-2-yne with **8**. A disadvantage of **8** lies in its higher steric congestion slowing down its exchange reactions; in extreme, it did not react with bulky 1-*t*-butyl-2-(trimethylsilyl)ethyne at all. Compound **1** also occurred to be less sterically limited than **8** in reactions with 1,4-disubstituted 1,3-diynes; however, it was reluctant to react with the highly sterically hindered triple bond of 2,4-di-tert-butylbut-1-ene-3-yne. Surprisingly, internal alkynes bearing a bulky *t*-butyl or isopropyl group in addition to methyl undergo isomerization upon coordination to titanocene to give allene complexes **11** and **12**. In distinction, pent-2-yne gave rise to titanocene-allene complex **13** only partially, whereas no allene complex could be detected for 1-phenylpropyne. It can be assumed that electron-donating bulky substituents are capable of inducing the above alkyne-allene isomerization. The physico-chemical data for acetylene complexes **3–10**, such as infrared ν(C≡C) vibration and ^{13}C NMR resonances for acetylenic carbon atoms δ(C≡C) gathered in Table 1 together with the X-ray crystallographic Ti–C and C≡C bond lengths do not unequivocally correlate with the electron-induction effect of the acetylene substituents. A good correlation was found only for the longest-wavelength electronic absorption band displayed by compounds **3–9** in the range 670–920 nm. This band was assigned to the HOMO-LUMO transition on the basis of DFT calculations which showed that the first excitation involves predominantly a $b_2 \rightarrow 1a_1$ transition. The computed first excitation energies for **3–9** followed the order of hypsochromic shifts of the absorption band relative to **8** that were induced by acetylene substituents: Me > Ph >> $SiMe_3$. The first excitation energies follow the order of Counterpoise energies of interaction of bent titanocene and bent alkyne fragments and correlate well with optimized averaged Ti–C bond lengths, implying that a shorter experimental λ_{max} results from a stronger alkyne coordination. The

Lauher-Hoffmann model , assuming back-bonding in the titanocene(Ti^{II})-ethene complex[2] appeared to be applicable for the above alkyne complexes.

Experimental

General considerations

All reactions leading to low-valent titanium compounds and their subsequent reactions were carried out on a vacuum line in sealed all-glass devices equipped with breakable seals. ^{1}H (300 MHz), ^{13}C (75 MHz) and ^{29}Si (59.6 MHz) NMR spectra were recorded on a Varian Mercury 300 spectrometer in toluene-d_8 solutions at 25 °C. Chemical shifts (δ/ppm) are given relative to the residual solvent signal (CD_2H: δ_H 2.08 ppm) and the solvent resonance (C_{ipso}: δ_C 137.48 ppm). The δ_{Si} values are related to external tetramethylsilane. EI-MS spectra were obtained on a VG-7070E mass spectrometer at 70 eV. Crystalline samples in sealed capillaries were opened and inserted into the direct inlet under argon. The spectra are represented by the peaks of relative abundance higher than 7 % and by important peaks of lower intensity. Crystalline samples for EI-MS measurements and melting point determinations were placed in glass capillaries, and KBr pellets were prepared in a glovebox Labmaster 130 (mBraun) under purified nitrogen (concentrations of oxygen and water were lower than 2.0 ppm) and sealed with flame. IR spectra of samples in KBr pellets prepared in the glovebox were measured in an air-protecting cuvette on a Nicolet Avatar FT IR spectrometer in the range 400–4000 cm^{-1}. UV-near IR spectra in the range 300–2000 nm were measured on a Varian Cary 17D spectrometer in all-sealed quartz cells (Hellma). Elemental analyses were carried out on a FLASH EA1112 CHN/O Automatic Elemental Analyzer (Thermo Scientific). Melting points were measured on a Koffler block in sealed glass capillaries under nitrogen, and are uncorrected.

Chemicals

The solvents tetrahydrofuran (THF), hexane, and toluene were dried by refluxing over $LiAlH_4$ and stored as solutions of green dimeric titanocene [(μ-η^5:η^5-

$C_5H_4C_5H_4)(\mu\text{-}H)_2\{Ti(\eta^5\text{-}C_5H_5)\}_2]$.[34] Toluene-$d_8$ C_7D_8 (99.5 % D) (Sigma Aldrich) was degassed, distilled under vacuum on singly tucked-in permethyltitanocene $[Ti(C_5Me_5)(C_5Me_4CH_2)]$,[7b] and stored as its solution on a vacuum line. The titanocene dichloride $[TiCl_2(\eta^5\text{-}C_5Me_5)_2]$ (Sigma Aldrich) was degassed before use. Internal alkynes but-2-yne, pent-2-yne, hex-3-yne, 1-phenylpropyne, 1-(trimethylsilyl)propyne, 1-*tert*-butylpropyne, 1-isopropylpropyne, 1,2-diphenylethyne, 1-(trimethylsilyl)-2-phenylethyne, 1-*tert*-butyl-2-(trimethylsilyl)ethyne, and bis(trimethylsilyl)acetylene (BTMSA), and 1,4-bis(trimethylsilyl)buta-1,3-diyne, 1,4-diphenylbuta-1,3-diyne, and 2,2,7,7-tetramethylocta-3,5-diyne (all Sigma Aldrich) were degassed and handled in vacuum. Head-to-tail dimers of (trimethylsilyl)ethyne and *tert*-butylethyne, 2,4-bis(trimethylsilyl)but-1-ene-3-yne and 2,4-di-*tert*-butylbut-1-ene-3-yne were obtained catalytically.[35] Ethene (polymerization grade) was obtained from Polymer Institute Brno (Czech Republic). It was degassed at liquid nitrogen temperature, then dosed by distilling on a vacuum line. Magnesium turnings (purum for Grignard reaction) (Sigma Aldrich) were used as received. The ethene complex $[Ti(II)(\eta^2\text{-}C_2H_4)(\eta^5\text{-}C_5Me_5)_2]$ (**1**) was obtained from $[TiCl_2(\eta^5\text{-}C_5Me_5)_2]$ by reducing it with magnesium in THF in the presence of excess ethene.[4]

Synthesis

Preparation of 3. A suspension of degassed **1** (0.346 g, 1.0 mmol) in hexane (10 mL) was mixed with PhC≡CPh (0.178 g, 1.0 mmol) in a 50 mL ampoule, and the mixture was stirred at 60 °C for 20 min. A greenish-yellow solution was concentrated to about a half volume by pumping off ethene and hexane into a liquid nitrogen-cooled trap. The solution was then heated again to 60 °C for 20 min, and partly evaporated to vacuum once more to get a nearly saturated solution. This was placed into a refrigerator (−5 °C) so that the solvent slowly distilled to an arm close to a cooler wall of a refrigerator yielding a crystalline green solid. Some residual mother liquor (ca. 0.3 mL) was poured to the arm containing the solvent, and the solid product was dissolved in a minimum of hexane distilled back. The crystallization in the above way was repeated. The arm containing impurities and the solvent was cooled with liquid nitrogen and sealed off. The arm containing a green crystalline

product was opened in a glovebox, the product weighed, and distributed for determination of melting point, EI-MS, IR, and ^{1}H and ^{13}C NMR spectra, and X-ray crystal structure determination and elemental analysis. Yield 0.44g (89%). Analytical data for **3** agreed with the reported ^{1}H and ^{13}C NMR and infrared spectra.[3,11a] Single crystal X-ray diffraction of the green crystals revealed the same unit cell as that reported for violet-brown crystals.[11a] Mp. 200 °C, EI-MS (180 °C): *m/z* (relative abundance) ($M^{\cdot+}$ 496 not observed), [Cp^*_2Ti]: 318 ($[M']^{+\cdot}$; 100), and its fragment peaks (as for **1** after ethene dissociation),[4] [PhC_2Ph]: 178 ($[M"]^{\cdot+}$; 85) - abundance was decreasing during evaporation. IR (KBr, cm^{-1}): 3068 (w), 3046 (vw), 3018 (vw), 2980 (m), 2902 (vs), 2856 (s), 2719 (vw), 1644 (s), 1587 (s), 1565 (w), 1482 (s), 1437 (m), 1377 (m), 1234 (w), 1153 (w), 1069 (w), 1025 (m), 908 (vw), 836 (vw), 760 (vs), 694 (s), 596 (vw), 545 (vw), 421 (s). UV–near IR (hexane, nm): 350 (sh) > 405 >> 560 > 710. Found (%): C, 82.28; H, 8.14. $C_{34}H_{40}Ti$ requires (%): C, 82.24; H, 8.12.

Preparation of 4. Compound **1** (0.346 g, 1.0 mmol) in hexane (10 mL) was reacted with MeC≡CPh (0.125 g, 1.08 mmol) following the procedure for obtaining **3**. Recrystallisation of the crude brown product gave brownish green crystals. Yield 0.37 g (85%).

Analytical data for compound **4**: Mp: 125 °C dec. ^{1}H NMR (toluene-d_8): 1.70 (s, 30H, $C_5\mathit{Me}_5$); 1.92 (s, 3H, ≡C*Me*); 6.47-6.53 (m, 2H, CH_{orho}, *Ph*); 6.88 (t, $^{3}J_{HH}$ = 7.5 Hz , 1H, CH_{para}, *Ph*); 7.03-7.08 partially overlapped by solvent signal (m, 2H, CH_{meta}, *Ph*). ^{13}C {^{1}H}(toluene-d_8): 12.04 ($C_5\mathit{Me}_5$); 19.68 (≡C*Me*); 121.27 (C_5Me_5); 124.42, 128.09, 129.79 (*C*H, *Ph*); 141.14 (C_{ipso}, *Ph*); 192.77 (≡*C*Ph); 207.66 (≡*C*Me). EI-MS(120 °C): *m/z* (relative abundance) ($M^{\cdot+}$ 434 not observed), [Cp^*_2Ti]: 318 ($[M']^{\cdot+}$; 100), and its fragment peaks; [MeC_2Ph]: 117 (29), 116 ($[M"]^{\cdot+}$; 66), 115 (87), 91 (33), abundances of *m/z* 115-117 peaks change during evaporation in favor of *m/z* 117, and observation of growing peaks with *m/z* 433 and 549 indicates the sample decomposition. IR (KBr, cm^{-1}): 3066 (vw), 3052 (vw), 3018 (vw), 2976 (m), 2902 (vs), 2856 (s), 2719 (vw), 1664 (s), 1585 (m), 1546 (vw), 1480 (m), 1438 (m,b), 1377 (s), 1212 (vw), 1164 (vw), 1068 (w), 1024 (m), 905 (vw), 804 (vw), 756 (s), 694 (s), 666 (w), 566 (vw), 505 (vw), 423 (s). UV–near IR (hexane, nm): 330 > 405(sh) >> 555 ~ 705. Found (%): C, 80.20; H, 8.79. $C_{29}H_{38}Ti$ requires (%): C, 80.16; H, 8.82.

Preparation of 5. Compound **1** (0.346 g, 1.0 mmol) in hexane (10 mL) was reacted with MeC≡CSiMe$_3$ (0.120 g, 1.07 mmol) following the procedure for obtaining **3** except that all volatiles were removed to vacuum, then toluene (5 mL) and the alkyne (0.120 g, 1.07 mmol) were added to the residue, and this mixture was heated again to 60 °C for 20 min. All volatiles were evaporated, and a crude brown product was purified by crystallisation from hexane. Brownish green crystals forming thin-plate aggregates were obtained after recrystallisation. Yield 0.38 g (88%).

Analytical data for **5**: Mp: 174 °C. ^{1}H NMR (toluene-d_8): 0.06 (s, 9H, Si*Me*$_3$); 1.57 (s, 3H, ≡C*Me*); 1.69 (s, 30H, C$_5$*Me*$_5$). ^{13}C {^{1}H}(toluene-d_8): 3.32 (Si*Me*$_3$); 12.22 (C$_5$*Me*$_5$); 20.48 overlapped by solvent signal (≡C*Me*); 120.98 (*C*$_5$Me$_5$); 206.60 (≡*C*Me); 232.19 (≡*C*SiMe$_3$). ^{29}Si {^{1}H}(toluene-d_8): −15.1 (*Si*Me$_3$). EI-MS(150 °C): *m/z* (relative abundance) (M$^{\cdot+}$ 430 not observed), [Cp*$_2$Ti]: 318 ([M']$^{\cdot+}$; 100), and its fragment peaks; [MeC$_2$SiMe$_3$]: 112 ([M"]$^{\cdot+}$; 10). IR (KBr, cm^{-1}): 2947 (s), 2904 (vs), 2857 (m), 2720 (vw), 1632 (s), 1502 (w), 1434 (m,b), 1377 (s), 1240 (s), 1056 (w), 1022 (m), 975 (w), 941 (vw), 844 (vs), 830 (s), 750 (w), 707 (w), 678 (m), 617 (vw), 597 (vw), 581 (w), 508 (vw), 425 (s). UV−near IR (hexane, nm): 390 >>> 515 < 775. Found (%): C, 72.51; H, 9.80. C$_{26}$H$_{42}$SiTi requires (%): C, 72.53; H, 9.83.

Preparation of 6. Compound **1** (0.346 g, 1.0 mmol) in hexane (10 mL) was reacted with PhC≡CSiMe$_3$ (0.180 g, 1.03 mmol) following the procedure for obtaining **5** except that heating to 60 °C lasted 1 h. Recrystallisation of a crude brown product afforded yellow-brown crystals. Yield 0.46 g (93%).

Analytical data for compound **6**: Mp: 152 °C. ^{1}H NMR (toluene-d_8): 0.17 (s, 9H, Si*Me*$_3$); 1.71 (s, 30H, C$_5$*Me*$_5$); 6.28 (d, $^3J_{HH}$ = 7.5 Hz , 2H, C*H*$_{orho}$, *Ph*); 6.85 (t, $^3J_{HH}$ = 7.2 Hz , 1H, C*H*$_{para}$, *Ph*); 6.96-7.02 partially overlapped by solvent signal (m, 2H, C*H*$_{meta}$, *Ph*). ^{13}C {^{1}H}(toluene-d_8): 3.57 (Si*Me*$_3$); 12.60 (C$_5$*Me*$_5$); 121.80 (*C*$_5$Me$_5$); 125.95, 127.80, 131.03 (*C*H, *Ph*); 139.10 (*C*$_{ipso}$, *Ph*); 213.21 (≡*C*Ph); 224.48 (≡*C*SiMe$_3$). ^{29}Si {^{1}H}(toluene-d_8): −17.1 (*Si*Me$_3$). EI-MS(150 °C): *m/z* (relative abundance) (M$^{\cdot+}$ 492 not observed), [Cp*$_2$Ti]: 318 ([M']$^{\cdot+}$; 100), and its fragment peaks; [PhC$_2$SiMe$_3$]: 174 ([M"]$^{\cdot+}$; 7), 159 ([M − Me]$^+$; 63), 73 ([SiMe$_3$]$^+$; 19). IR (KBr, cm^{-1}): 3087 (vw), 3074 (vw), 3042 (w), 2976 (m), 2948 (s), 2898 (vs), 2857 (m), 2721 (vw), 1621 (s), 1588 (m), 1567 (w), 1496 (w),1481 (m), 1439 (m), 1376 (s),

1253 (m), 1242 (s), 1186 (w), 1164 (w), 1069 (w), 1025 (m), 870 (s), 833 (vs), 763 (s), 753 (m), 698 (m), 677 (w), 649 (w), 589 (vw), 503 (vw), 449 (w), 422 (m). UV–near IR (hexane, nm): 327 (sh) > 370 (sh) > 410 (sh) >>> 535 < 780. Found (%): C, 75.55; H, 8.96. $C_{31}H_{44}SiTi$ requires (%): C, 75.58; H, 9.00.

Preparation of 7. Compound **1** (0.346 g, 1.0 mmol) in hexane (20 mL) was mixed with *t*-BuC≡CSiMe$_3$ (0.23 g, 1.5 mmol) in a large ampoule (100 mL) and heated to 60 °C for 6 h. Then, the evolved ethene was pumped off together with some hexane; the ampoule was then sealed and heated again to 60 °C for 6 h. All the volatiles were evaporated in vacuum at 60 °C, and the residue was dissolved in 5 mL of hexane. Cooling to −5 °C afforded a crop of ocher crystals. The mother liquor was further concentrated to half of its volume, the crystallisation was repeated, which afforded another crop of crystals of the same appearance. The combined yield of dry crystals was 0.40 g (86%).

Analytical data for **7**: Mp: 130 °C dec. ^{1}H NMR (toluene-d_8): 0.04 (s, 9H, Si*Me*$_3$); 0.91 (s, 9H, C*Me*$_3$); 1.80 (s, 30H, C$_5$*Me*$_5$). ^{13}C {^{1}H}(toluene-d_8): 5.20 (Si*Me*$_3$); 13.18 (C$_5$*Me*$_5$); 33.64 (C*Me*$_3$); 43.71 (*C*Me$_3$); 122.03 (*C*$_5$Me$_5$); 212.06 (≡*C*CMe$_3$); 242.35 (≡*C*SiMe$_3$). ^{29}Si {^{1}H}(toluene-d_8): −19.6. EI-MS (150 °C): *m/z* (relative abundance) ($M^{\cdot+}$ 472 not observed), [Cp*$_2$Ti]: 318 ([M']$^{\cdot+}$; 100), and its fragment peaks; [Me$_3$CC$_2$SiMe$_3$]: 154 ([M"]$^{\cdot+}$; 24), 139 ([M − Me]$^+$; 100), 73 ([SiMe$_3$]$^+$; 28). IR (KBr, cm^{-1}): 2987 (m,sh), 2963 (s), 2903 (vs), 2860 (m), 2719 (vw), 1609 (s), 1444 (m,b), 1378 (s), 1354 (w), 1240 (s), 1210 (m), 1061 (vw), 1021 (w), 910 (s), 842 (vs), 752 (w), 663 (m), 599 (w), 589 (vw), 428 (s). UV–near IR (hexane, nm): 330(sh) > 402 >>> 530 < 850. Found (%): C, 73.71; H, 10.27. $C_{29}H_{48}SiTi$ requires (%): C, 73.69; H, 10.24.

Preparation of 8. Compound **1** (0.346 g, 1.0 mmol) in toluene (10 mL) was mixed with BTMSA (0.4 mL, 1.8 mmol) under vacuum in a large ampoule (100 mL) and heated to 60 °C for 6 h. Then, the evolved ethene was pumped off together with some toluene, and the ampule was sealed out and heated again to 60 °C for 6 h. All the volatiles were evaporated in vacuum at 60 °C, then toluene (3 mL) and BTMSA (0.2 mL, 0.9 mmol) were added to the residue. This mixture was heated to 60 °C for 6 h, and then all volatiles were evaporated under vacuum at 60 °C. A yellow crystalline

residue was dissolved in toluene-d_8 and analysed by ^{1}H and ^{13}C NMR spectra to be **8** containing about 2% of **1**.

Reaction of 8 with ethene in a sealed NMR tube. A solution of of **8** in toluene-d_8 (0.15 mmol in 1.0 mL) was transferred into an NMR tube, some gaseous ethene was condensed under cooling with liquid nitrogen, and the tube was sealed off with flame. The ^{1}H NMR spectrum, taken after 3 h at room temperature assessed the molar composition **8** 35% and ethene 65%. After heating the tube to 60 °C for 8 h followed by keeping at room temperature for 2 weeks the composition was **8** 18%, ethene 34%, BTMSA 17%, and **1** 31%. It corresponded to the equilibrium constant K = 0.86. This composition did not change during next 6 months within the peak integration error, however, new signals of 1,3-butadiene and ethane were growing in intensity within next 6 months. This implies very slow ethene consumption as described earlier.[1]

Reaction of 8 with internal alkynes to give 3–6 and 9, and 10, respectively, as analysed by ^{1}H NMR spectra.[a] Complex **8** in toluene-d_8 (0.15 mmol/1.0 mL) was mixed under vacuum with a molar excess of alkyne, and this mixture was transferred into an NMR tube which was cooled with liquid nitrogen before it was sealed off with flame. The initial sum of integrals of resonances of **8** and the respective alkyne was used to calculate the initial molar percentage (the first line); integrals of known resonances for free BTMSA and the formed complexes **3–10** were analogously used to calculate the final composition (second line). This was achieved for **3–6** and **10** after heating to 80 ºC for 7 h followed by keeping at room temperature for 5 days. Complex **7** refused to form even after heating to 100 ºC for 3 h; after heating to 110 ºC for 7 h, a small part of **8** was converted to doubly tucked-in titanocene [Ti(C_5Me_5)($C_5Me_3(CH_2)_2$]). But-2-yne was reacted with **8** to give **9** at room temperature; the initial composition, the composition after 4 weeks, and after 7 weeks are given.

Complex	[**8**], %	Alkyne, %	BTMSA, %	Complex,%
3	30	70	0	0
3	0	36	32	32

4	40	60	0	0
4	0	20	40	40
5	16	84	0	0
5	0	68	16	16
6	23	77	0	0
6	0	53	23	23
7	32	68	0	0
7	27[b]	68	0	0
9[b]	18	82	0	0
9[b]	1	65	17	17
9[b,c]	0	64	18	18
10	17	83	0	0
10[d]	0	66	17	17

[a] Precision of the ^{1}H NMR resonance integral ~ 2–10%. [b] NMR analysis after 3 h at room temperature (1-st line), after 4 weeks (2-nd line), and after 7 weeks at room temperature 20–25 °C (3-rd line). [c] Data for **9** in toluene-d_8 are as follows. ^{1}H NMR: 1.56 (s, 6H, ≡C*Me*); 1.68 (s, 30 H, C_5*Me*$_5$). ^{13}C NMR: 11.8 (C_5*Me*$_5$); 17.4 (≡C*Me*); 120.6 (*C*$_5$Me$_5$); 200.7 (≡*C*Me). Their difference from the reported data[3] is due to the different solvent (cyclohexane-d_{12}). [d] ^{1}H and ^{13}C NMR data for **10** in toluene-d_8 agree with those reported for benzene-d_6 solution.[11a]

Preparation of 11. Compound **1** (0.346 g, 1.0 mmol) in hexane (10 mL) was reacted with MeC≡CCMe$_3$ (0.45 g, 4.7 mmol) in a large ampoule (100 mL) at 25 °C. After 1 day stirring all volatiles were evaporated in vacuum, and a green crystalline residue was dissolved in 3.0 mL of hexane. Crystallisation with a slow distillation of the solvent in a refrigerator afforded a green crystalline solid. This was recrystallised to give green crystals. Yield 0.36 g (87%).

Analytical data for **11**: Mp: 107 °C. ^{1}H NMR (toluene-d_8): 1.05 (s, 9H, C*Me*$_3$); 1.63 (s, 30H, C$_5$*Me*$_5$); 2.03 (d, $^{4}J_{HH}$ = 3.3 Hz, 2H, =C*H*$_2$); 3.50 (t, $^{4}J_{HH}$ = 3.3 Hz, 1H, =C*H*). ^{13}C {^{1}H}(toluene-d_8): 11.80 (C$_5$*Me*$_5$); 30.93 (C*Me*$_3$); 35.79 (*C*Me$_3$); 84.66 (=C*H*$_2$); 119.03 (*C*$_5$Me$_5$); 128.30 (=*C*H); 231.20 (C=*C*=C). EI-MS (90 °C): *m/z* (relative abundance) 414 ($M^{+\cdot}$; 0.5), [Cp*$_2$Ti]: 318 ([M'] $^{\cdot+}$; 100), and its fragment peaks;

[Me_3CC_2Me]: 96 ([M"]$^{\cdot+}$; 4), 81 ([M" – Me]$^+$; 10), 57 ([Bu]$^+$; 18). IR (KBr, cm^{-1}): 2955 (s), 2940 (m), 2901 (vs), 2858 (m), 2721 (vw), 1650 (vw), 1488 (w), 1454 (m), 1432 (m), 1378 (s), 1355 (m), 1245 (m), 1197 (w), 1163 (vw), 1064 (vw), 1022 (m), 966 (vw), 873 (w), 828 (w), 804 (vw), 752 (vw), 669 (w), 501 (vw), 424 (s). UV–near IR (hexane, nm): 362(sh) >>> 545 < 665(sh) < 770. Found (%): C, 78.26; H, 10.17. $C_{27}H_{42}Ti$ requires (%): C, 78.24; H, 10.21.

Preparation of 12. Compound **1** (0.346 g, 1.0 mmol) in hexane (10 mL) was reacted with 4-methylpent-2-yne MeC≡CCHMe_2 (0.5 mL, 4.2 mmol) in a large ampoule (100 mL) at 25 °C. After 1 day all volatiles were evaporated in vacuum, and a dirty green oily residue was dissolved in 2.0 mL of hexane. Attempts to purify the product by crystallisation were unsuccessful. The solution (0.4 mL) was evaporated in vacuum to give brownish-green oil which solidified in a refrigerator. The content of **12** was at least 85% as analysed by ^{1}H and ^{13}C NMR; the byproducts were not identified.
Analytical data for compound **12**: ^{1}H NMR (toluene-d_8): 1.04 (d, $^3J_{HH}$ = 6.6 Hz, 6H, CHMe_2); 1.64 (s, 30H, C_5Me_5); 2.01-2.11 (m, 1H, C$H$$Me_2$); 2.17 (d, $^4J_{HH}$ = 2.4 Hz, 2H, =CH_2); 3.64 (dt, $^3J_{HH}$ = 5 Hz, $^4J_{HH}$ = 2.4 Hz, 1H, =CH). ^{13}C {^{1}H}(toluene-d_8): 11.83 (C_5Me_5); 23.88 (CHMe_2); 35.35 (CHMe_2); 86.38 (=CH_2); 119.05 (C_5Me$_5$); 127.48 (=CH); 234.56 (C=C=C).

Preparation of 13. Pent-2-yne (0.5 mL, 5.2 mmol) was added to a solution of **1** (0.346 g, 1.0 mmol) in 10 mL of hexane and after warming to 60 °C for 1 h all volatiles were evaporated under vacuum. A greenish brown oil was analyzed by ^{1}H and ^{13}C NMR spectra to contain 35% of **13** and 65% of the alkyne complex [Ti(η^2-MeC≡CEt) (η^5-C_5Me_5)$_2$] (**13A**) in addition to the non-identified byproducts.
Analytical data for compound **13**: ^{1}H NMR (toluene-d_8): 1.04 (d, $^3J_{HH}$ = 6.6 Hz, 3H, =CHMe); 1.66 (s, 30H, C_5Me_5); 2.16-2.22 (m, 2H, =CH_2); 3.79-3.90 (m, 1H, =CH). ^{13}C {^{1}H}(toluene-d_8): 11.90 (C_5Me_5); 15.40 =CHMe); 86.90 (=CH_2); 119.12 (C_5Me$_5$); 121.90 (=CH); 237.05 (C=C=C).
Analytical data for compound **13A**: ^{1}H NMR (toluene-d_8): 0.97 (t, $^3J_{HH}$ = 6.3 Hz, 3H, CH_2Me); 1.62 (s, 3H, ≡CMe); 1.71 (s, 30H, C_5Me_5); 1.90 (q, $^3J_{HH}$ = 6.3 Hz, 2H, CH_2Me). ^{13}C {^{1}H}(toluene-d_8): 11.94 (C_5Me_5); 15.48 (CH_2Me); 18.61 (≡CMe); 27.89 (CH$_2$Me); 120.53 (C_5Me$_5$); 196.91 (≡CMe); 201.13 (≡CCH$_2$).

Preparation of 15. Compound **1** (0.346 g, 1.0 mmol) in hexane (10 mL) was reacted with $Me_3SiC{\equiv}CC{\equiv}CSiMe_3$ (0.39 g, 2.0 mmol) in a large ampoule (100 mL) at 25 °C for 10 h. Then, all volatiles were evaporated in vacuum, and a brown residue was dissolved in 5 mL of hexane, and crystallised at −28 °C. Large red (or green) crystals obtained were recrystallised from the saturated solution in hexane to give red crystals. Yield 0.42 g (82%). ^{1}H and ^{13}C NMR data agree with ref.[23a].

Additional data for compound **15**: Mp: 124 °C. EI-MS (110 °C): *m/z* (relative abundance) 513 (6), 512 ($M^{+\cdot}$; 13), 439 ($[M - SiMe_3]^+$; 2), 320 (12), 319 (31), 318 ($[M - C_4(SiMe_3)_2]^+$; 100), 317 (47), 316 (17), 315 (8), 182 (6), 181 (17), 180 (10), 179 (11), 178 (11), 177 (7), 133 (6),119 (9), 105 (7), 91 (8), 73 ($[SiMe_3]^+$; 20). IR (KBr, cm^{-1}): 2950 (s,), 2901 (s), 2857 (m), 2720 (vw), 2092 (s), 2050 (sh), 1609 (m), 1494 (w,b), 1445 (m,b), 1403 (vw), 1378 (m), 1309 (vw), 1240 (s), 1158 (vw), 1064 (vw), 1024 (m), 848 (vs), 755 (m), 730 (w), 622 (w), 502 (w), 436 (m). UV−vis (hexane, nm): 330 (sh) > 405 (sh) >> 515 (sh) > 710.

Preparation of 16. Compound **1** (0.346 g, 1.0 mmol) in hexane (10 mL) was reacted with PhC≡CC≡CPh (0.30 g, 1.5 mmol) in a large ampoule (100 mL) at 40 °C for 2 h affording a green solution. All volatiles were evaporated in vacuum, and a green residue was dissolved in warm hexane (10 mL). Crystallisation at −5 °C afforded a green finely crystalline solid. Mother liquor containing the unreacted diyne was separated, and the product was washed with condensing hexane vapor, and dried in vacuum. Yield 0.38 g (74%). ^{1}H and ^{13}C NMR data agree with those reported for benzene-d_6 solution.[23a]

Additional data for compound **16**: Mp: 155 °C. EI-MS (130 °C): *m/z* (relative abundance) 523 (13), 522 (47), 521 (59), 520 ($M^{+\cdot}$; 100), 519 (48), 518 (46), 517 (9), 516 (11), 507 (12), 506 ($[M - CH_2]^+$; 25), 505 ($[M - Me]^+$; 12), 504 ($[M - CH_4]^+$; 18), 503 (23), 491 (12), 490 ($[M - 2\,Me]^+$; 25), 489 (7), 429 ($[M - PhCH_2]^+$; 9), 260 ($[M]^{2+}$; 13), 250 (7), 221 (13), 182 (14), 181 (21), 180 (11), 179 (10), 178 (16), 177 (11), 176 (9), 119 (9), 105 (7), 91 (19), 77 (7). IR (KBr, cm^{-1}): 3081 (vw), 3047 (w,b), 3015 (w), 2976 (m), 2906 (vs), 2856 (m), 2720 (vw), 1612 (m), 1595 (s), 1570 (w), 1490 (s), 1470 (m), 1440 (s), 1376 (s), 1354 (w), 1309 (vw), 1245 (w,b), 1155 (w), 1103 (vw), 1075 (w), 1022 (m), 915 (w), 883 (vw), 861 (vw), 851 (w), 815 (m), 765

(w), 753 (s), 708 (s), 695 (vs), 611 (vw), 583 (vw), 570 (w), 556 (vw), 505 (m), 483 (w), 429 (m). UV−near IR (hexane, nm): 640.

Preparation of 17. Compound **1** (0.346 g, 1.0 mmol) in hexane (10 mL) was reacted with *t*-BuC≡CC≡C*t*-Bu (0.20 g, 1.2 mmol) in a large ampoule (100 mL) at 40 °C for 2 h affording a green solution. All volatiles were evaporated in vacuum; at final 100 °C yielding several colorless crystals of the sublimed excessive butadiyne. A brown residue was dissolved in toluene-d_8. Its ^{1}H and ^{13}C NMR spectra revealed the overwhelming presence of **17** contaminated with the initial diyne and some non-identified impurities. All resonances reported for **17** in benzene-d_6[23b] were found.

Preparation of 18. Compound **1** (0.346 g, 1.0 mmol) in hexane (10 mL) was reacted with freshly vacuum-distilled $Me_3SiC{\equiv}CC(SiMe_3){=}CH_2$ (0.26 g, 1.3 mmol) at 60 °C for 3 h. Then, the reaction ampoule was opened to vacuum, and ethene and some hexane were evaporated. The ampoule was sealed with flame and heated to 60 °C for another 3 h. The formed ethene was again pumped to vacuum and the solution concentrated to saturation. Its cooling in a refrigerator afforded a crop of ocher crystalline solid. This was washed with condensing hexane vapor, and recrystallised from hexane. Yield 0.48 g (94%). Data for **18** including the crystallographic unit cell agree with those reported.[23c]

Unsuccessful treatment of 1 with *t*-BuC≡CC(*t*-Bu)=CH$_2$. Freshly vacuum-distilled *t*-BuC≡CC(*t*-Bu)=CH$_2$ (0.33 g, 2.0 mmol) was added to **1** (0.346 g, 1.0 mmol) suspended in hexane (10 mL), and the mixture was heated to 60 °C for 3 days. No reaction proceeded; unchanged **1** was isolated after evaporation of all volatiles in vacuum.

X-Ray crystallography

Single crystals or crystal fragments of **4**, **6**, **7**, and **11** were mounted into Lindemann glass capillaries in a Labmaster 130 glovebox (mBraun) under purified nitrogen. Diffraction data for all complexes were collected on a Nonius KappaCCD diffractometer (MoK_α radiation, λ = 0.71073 Å) equipped with an APEX II area

detector. The raw data were processed by the APEX2 program package.[36] The phase problem was solved by direct methods (SIR97),[37] followed by consecutive Fourier syntheses and refined by full-matrix least-squares on F^2 (SHELXL-97).[38] The pseudomerohedral twinning of **7** was accounted for in the refinement using the twinning matrix –1 0 0, 0 –1 0, 0 0 1 and a batch factor 0.322. Relevant crystallographic data are gathered in Supplementary Information. All non-hydrogen atoms were refined anisotropically. The C–H hydrogen atoms were put into idealised positions (riding model), and assigned temperature factors either $H_{iso}(H) = 1.2U_{eq}$(pivot atom) or $H_{iso}(H) = 1.5U_{eq}$(pivot atom), except for hydrogen atoms of phenyl rings in **4** H(25–29) and **6** H(24–28), and H(21A), H(21B), and H(23) of **11**. These were refined isotropically without any restraints. Molecular graphics were obtained with a recent version of the PLATON program.[39]

Computational details

DFT studies have been carried out at the *fermi* and *bose* clusters at the J. Heyrovský Institute of Physical Chemistry, Academy of Sciences of Czech Republic, v.v.i., using Gaussian 09, Revision C.01 and D.01.[40] All computations used the M06 functional. The molecules were optimised using the 6-31G(d,p) basis set employed for all atoms and an analytical Hessian computed before the first step of the optimization procedure. Natural Bonding Analysis[41] was carried out by the NBO 5.G program.[42] The electronic transitions were computed by time-dependant DFT against the optimised geometries using the 6-311++G(2d,p) basis set for all atoms, an ultrafine integration grid and the Douglas-Kroll-Hess Hamiltonian. Visualization and examination of molecular orbitals was accomplished by Molden.[43]

Acknowledgements

This research was supported by Grant Agency of the Czech Republic (Project No. P207/12/2368). R.Gy. is grateful to the Slovak Grant Agency VEGA (Project No. 1/0336/13).

Notes and references

1 S. A. Cohen, P. R. Auburn and J. E. Bercaw, *J. Am. Chem. Soc.*, 1983, **105**, 1136-1143.

2 J. W. Lauher and R. Hoffmann, *J. Am. Chem. Soc.*, 1976, **98**, 1729-1742.

3 S. A. Cohen and J. E. Bercaw, *Organometallics*, 1985, **4**, 1006-1014.

4 J. Pinkas, I. Císařová, R. Gyepes, J. Kubišta, M. Horáček and K. Mach, *Organometallics*, 2012, **31**, 5478-5493.

5 V. Burlakov, U. Rosenthal, P. V. Petrovskii, V. B. Shur and M. E. Vol'pin, *Metalloorg. Khim.*, 1988, **1**, 953-954.

6 (*a*) U. Rosenthal, V. V. Burlakov, P. Arndt, W. Baumann and A. Spannenberg, *Organometallics*, 2003, **22**, 884-900; (*b*) U. Rosenthal, V. V. Burlakov, P. Arndt, W. Baumann, A. Spannenberg and V. B. Shur, *Eur. J. Inorg. Chem.*, 2004, 4739-4749; (*c*) U. Rosenthal and V. V. Burlakov, in *Titanium and Zirconium in Organic Synthesis*, ed. I. Marek, Wiley-VCH, Weinheim, Germany, 2002, pp. 355-389.

7 (*a*) K. Mach, R. Gyepes, J. Kubišta and M. Horáček, *Inorg. Chem. Commun.*, 2006, **9**, 156-159; (*b*) J. Pinkas, I. Císařová, R. Gyepes, M. Horáček, J. Kubišta, J. Čejka, S. Gómez-Ruiz, E. Hey-Hawkins and K. Mach, *Organometallics*, 2008, **27**, 5532-5547.

8 M. Horáček, V. Kupfer, U. Thewalt, P. Štepnička, M. Polášek and K. Mach, *Organometallics*, 1999, **18**, 3572-3578.

9 M. Polášek and J. Kubišta, *J. Organomet. Chem.*, 2007, **692**, 4073-4083.

10 V. Varga, K. Mach, M. Polášek, P. Sedmera, J. Hiller, U. Thewalt and S. I. Troyanov, *J. Organomet. Chem.*, 1996, **506**, 241-251.

11 (*a*) P. Arndt, V. V. Burlakov, A. Spannenberg and U. Rosenthal, *Inorg. Chem. Commun.*, 2007, **10**, 792-794. (*b*) V. V. Burlakov, A. V. Polyakov, A. I. Yanovsky, Y. T. Struchkov, V. B. Shur, M. E. Volpin, U. Rosenthal and H. Görls, *J. Organomet. Chem.*, 1994, **476**, 197-206.

12 (*a*) J. L. Templeton, *Adv. Organomet. Chem.*, 1989, **29**, 1-100; for Pt(0) (*b*) B. W. Davies and N. C. Payne, *Inorg. Chem.*, 1974, **13**, 1848-1853; (c) for Ni(0) (*c*) T. Bartik, B. Happ, M. Iglewsky, H. Bandmann, R. Boese, P. Heimbach, T. Hoffmann and E. Wenschuh, *Organometallics*, 1992, **11**, 1235-1241; for Co_2 complexes (*d*) B. Happ, T. Bartik, C. Zucchi, M. C. Rossi, F. Ghelfi, G. Palyi, G. Varadi, G. Szalontai, I. T. Horvath, A. Chiesivilla and C. Guastini, *Organometallics*, 1995, **14**, 809-819.

13 (*a*) J. Hiller, U. Thewalt, M. Polášek, L. Petrusová, V. Varga, P. Sedmera and K. Mach, *Organometallics*, 1996, **15**, 3752-3759. (*b*) T. Beweries, V. V. Burlakov, M. A. Bach, P. Arndt, W. Baumann, A. Spannenberg and U. Rosenthal, *Organometallics*, 2007, **26**, 247-249.

14 N. Nishina and Y. Yamamoto, *Angew. Chem. Int. Ed.*, 2006, **45**, 3314-3317.

15 J. W. Pattiasina, C. E. Hissink, J. L. Deboer, A. Meetsma and J. H. Teuben, *J. Am. Chem. Soc.*, 1985, **107**, 7758-7759.

16 K. Mashima, N. Sakai and H. Takaya, *Bull. Chem. Soc. Jpn.*, 1991, **64**, 2475-2483.

17 P. Binger, F. Langhauser, P. Wedemann, B. Gabor, R. Mynott and C. Kruger, *Chem. Ber.*, 1994, **127**, 39-45.

18 P. H. P. Brinkmann, G. A. Luinstra and A. Saenz, *J. Am. Chem. Soc.*, 1998, **120**, 2854-2861.

19 (*a*) M. W. Bouwkamp, J. de Wolf, I. D. Morales, J. Gercama, A. Meetsma, S. I. Troyanov, B. Hessen and J. H. Teuben, *J. Am. Chem. Soc.*, 2002, **124**, 12956-12957; (*b*) M. W. Bouwkamp, P. H. M. Budzelaar, J. Gercama, I. D. Morales, J. de Wolf, A. Meetsma, S. I. Troyanov, J. H. Teuben and B. Hessen, *J. Am. Chem. Soc.*, 2005, **127**, 14310-14319; (*c*) J. Pinkas, V. Varga, I. Císařová, J. Kubišta, M. Horáček and K. Mach, *J. Organomet. Chem.*, 2007, **692**, 2064-2070; (*d*) J. Pinkas, R. Gyepes, I. Císařová, J. Kubišta, M. Horáček and K. Mach, *Organometallics*, 2014, **33**, 3399-3413.

20 (*a*) S. C. Yu and S. M. Ma, *Chem. Commun.*, 2011, **47**, 5384-5418; (*b*) T. Bai, S. M. Ma and G. C. Jia, *Coord. Chem. Rev.*, 2009, **253**, 423-448.

21 (*a*) C. P. Casey and J. T. Brady, *Organometallics*, 1998, **17**, 4620-4629; (*b*) H. Werner, P. Schwab, N. Mahr and J. Wolf, *Chem. Ber.*, 1992, **125**, 2641-2650; (*c*) S. M. Coughlan and G. K. Yang, *J. Organomet. Chem.*, 1993, **450**, 151-155.

22 (*a*) D. L. Hughes, A. J. L. Pombeiro, C. J. Pickett and R. L. Richards, *J. Chem. Soc. Chem. Commun.*, 1984, 992-993. (*b*) T. B. Wen, Z. Y. Zhou, C. P. Lau and G. C. Jia, *Organometallics*, 2000, **19**, 3466-3468. (*c*) N. Phadke and M. Findlater, *Organometallics*, 2014, **33**, 16-18.

23 (*a*) P. M. Pellny, F. G. Kirchbauer, V. V. Burlakov, W. Baumann, A. Spannenberg and U. Rosenthal, *J. Am. Chem. Soc.*, 1999, **121**, 8313-8323; (*b*) P. M. Pellny, F. G. Kirchbauer, V. V. Burlakov, W. Baumann, A. Spannenberg and U. Rosenthal, *Chem. Eur. J.*, 2000, **6**, 81-90. (*c*) P. Štepnička, R. Gyepes, I. Císařová, M. Horáček, J. Kubišta and K. Mach, *Organometallics*, 1999, **18**, 4869-4880.

24 F. H. Allen, O. Kennard, D. G. Watson, L. Brammer, A. G. Orpen and R. Taylor, *J. Chem. Soc., Perkin Trans. 2*, 1987, S1-S19.

25 J. G. Yin, K. A. Abboud and W. M. Jones, *J. Am. Chem. Soc.*, 1993, **115**, 3810-3811.

26 (*a*) M. J. S. Dewar, *Bull. Soc. Chim. Fr.*, 1951, **18**, C79-C87; (*b*) J. Chatt and L. A. Duncanson, *J. Chem. Soc.*, 1953, 2939-2947.

27 G. Frenking and N. Fröhlich, *Chem. Rev.*, 2000, **100**, 717-774.

28 E. D. Jemmis, S. Roy, V. V. Burlakov, H. Jiao, M. Klahn, S. Hansen and U. Rosenthal, *Organometallics*, 2010, **29**, 76-81.

29 M. Horáček, J. Hiller, U. Thewalt, P. Štěpnička and K. Mach, *J. Organomet. Chem.*, 1998, **571**, 77-82.

30 (a) R. Gyepes, P. T. Witte, M. Horáček, I. Císařová and K. Mach, *J. Organomet. Chem.*, 1998, **551**, 207-213; (b) P. T. Witte, R. Klein, H. Kooijman, A. L. Spek, M. Polášek, V. Varga and K. Mach, *J. Organomet. Chem.*, 1996, **519**, 195-204.

31 (*a*) J. E. Bercaw and H. H. Brintzinger, *J. Am. Chem. Soc.*, 1971, **93**, 2045-2046; (*b*) K. Mach, V. Varga, V. Hanuš, and P. Sedmera, *J. Organomet. Chem.*, 1991, **415**, 87-95.

32 M. Horáček, P. Štěpnička, R. Gyepes, I. Císařová, I. Tišlerová, J. Zemánek, J. Kubišta and K. Mach, *Chem. Eur. J.*, 2000, **6**, 2397-2408.

33 (*a*) M. Horáček, P. Štěpnička, J. Kubišta, I. Císařová, L. Petrusová and K. Mach, *J. Organomet. Chem.*, 2003, **667**, 154-166. (*b*) P. M. Pellny, V. V. Burlakov, W. Baumann, A. Spannenberg, M. Horáček, P. Štěpnička, K. Mach and U. Rosenthal, *Organometallics*, 2000, **19**, 2816-2819; (*c*) L. Lukešová, P. Štěpnička, K. Fejfarová, R. Gyepes, I. Císařová, M. Horáček, J. Kubišta and K. Mach, *Organometallics*, 2002, **21**, 2639-2653; (*d*) J. Pinkas, L. Lukešová, R. Gyepes, I. Císařová, J. Kubišta, M. Horáček and K. Mach, *Organometallics*, 2010, **29**, 5199-5208.

34 H. Antropiusová, A. Dosedlová, V. Hanuš and K. Mach, *Trans. Met. Chem.*, 1981, **6**, 90-93.

35 (*a*) V. Varga, L. Petrusová, J. Čejka, V. Hanuš and K. Mach, *J. Organomet. Chem.*, 1996, **509**, 235-240; (*b*) V. Varga, L. Petrusová, J. Čejka and K. Mach, *J. Organomet. Chem.*, 1997, **532**, 251-259; (*c*) M. Horáček, I. Císařová, J. Čejka, J. Karban, L. Petrusová and K. Mach, *J. Organomet. Chem.*, 1999, **577**, 103-112.

36 Bruker, *APEX2, SAINT* (2010) Bruker AXS Inc., Madison, Wisconsin, USA.

37 A. Altomare, G. Cascarano, G. Giacovazzo, A. Guagliardi, M. C. Burla, G. Polidori and M. Camalli, *J. Appl. Crystallogr.*, 1994, **27**, 435-435.

38 G. M. Sheldrick, *SHELXL97, Program for Crystal Structure Refinement from Diffraction Data*, (1997) University Of Göttingen, Göttingen.

39 A. L. Spek, *PLATON, A Multipurpose Crystallographic Tool*, (2007) Utrecht University, Utrecht.

40 M. J. Frisch, et al., *Gaussian 09, Revision D.01*, (2009) Gaussian, Inc., Wallingford, CT, USA.

41 J. E. Carpenter and F. Weinhold, *J. Mol. Struct. (Theochem)*, 1988, **46**, 41-62.

42 E. D. Glendening, A. E. Reed, J. E. Carpenter and F. Weinhold, *NBO Version 3.1*, Theoretical Chemistry Institute, University of Wisconsin, Madison.

43 G. Schaftenaar and J. H. Noordik, *J. Comput.-Aided Mol. Des.*, 2000, **14**, 123-134.

Table 1 Selected ^{13}C NMR (δ, ppm) and IR (ν, cm^{-1}) data for [$Cp^*_2Ti(\eta^2\text{-}R^1C{\equiv}CR^2)$] complexes and free alkynes

Compound No.	R^1	R^2	δ(C≡C)[a] complex	δ(C≡C)[a] alkyne	Δδ(C≡C)	ν(C≡C) complex	ν(C≡C) alkyne	Δν(C≡C)	Ref.
3	Ph	Ph	200.6	90.1	110.5	1644	2223	579	1, 11a
4	Me	Ph	207.7, 192.8	85.9, 80.5	121.8, 112.3	1664	2233[b]	569	
5	Me	$SiMe_3$	206.6, 232.2	103.1, 83.9	103.5, 148.3	1632	2185	553	
6	Ph	$SiMe_3$	213.2, 224.5	106.1, 94.1	107.1, 130.4	1621	2160	539	11b
7	*t*-Bu	$SiMe_3$	212.1, 242.4	116.1, 82.2	96.0, 159.6	1609	2156	547	
8	$SiMe_3$	$SiMe_3$	248.5	114.0	134.5	1598[c]	2107	509	11b
9	Me	Me	200.1	74.3	125.8	1683	2240[d]	557	1
10	Et	Et	202.0	81.0	121.0	1678	2240[d]	562	11a
13A	Me	Et	196.9, 201.1	74.8, 80.7	122.1, 120.4	-	-	-	

[a] Measured in toluene-d_8. The signal assignment for asymmetrical alkynes and their complexes was done on the basis of gHMBC experiments. [b] Average value for the two observed absorption bands at 2250 cm^{-1} and 2216 cm^{-1} (Fermi resonance). [c] Center of gravity for the observed absorption bands: 1638(w), 1595(s), 1562(m).[10] [d] An estimated value, experimentally not observed symmetry-forbidden vibration.

Table 3 Selected bond lengths (Å) and bond angles (deg) for **3**[a], **4**, **6**, **7**, and **8**[b]

	3	**4**	**6**[c]	**7**[d]	**8**
Bond lengths (Å)					
Ti–Cg(1)[e]	-	2.1099(8)	2.0995(9)	2.1301(18)–2.1388(18)	-
Ti–Cg(2)[e]	-	2.0970(8)	2.1207(9)	2.1266(17)–2.1318(18)	-
Ti–Pl(1)[f]	-	2.1090(3)	2.0990(3)	2.1291(6)–2.1385(6)	-
Ti–Pl(2)[f]	-	2.0965(3)	2.1185(3)	2.1258(6)–2.1311(6)	-
Ti–C(a)[g]	2.103(3)	2.0899(18)	2.0786(19){2.089(2)}	2.098(3)–2.114(3)	2.122(3)
Ti–C(b)[g]	2.099(3)	2.0968(16)	2.123(2){2.139(2)}	2.111(3)–2.132(3)	2.126(3)
C(a)–C(b)[g]	1.306(4)	1.296(3)	1.302(3){1.308(3)}	1.292(5)–1.304(5)	1.309(4)
Bond angles (°)					
Cg(1)–Ti–Cg(2)[e]	-	141.08(3)	139.94(4)	135.42(6)–136.37(7)	-
C(a)–Ti–C(b)[g]	-	36.06(7)	36.10(8)	35.62(13)–35.89(13)	-
E(a)–C(a)–C(b)[g]	137.2(3)	138.39(17)	137.39(19){140.5(2)}	134.0(4)–137.0(3)	134.8(3)
E(b)–C(b)–C(a)[g]	137.6(3)	137.31(18)	139.53(17){138.1(2)}	137.8(3)–140.2(3)	136.8(3)
Dihedral angles (°)					
φ[h]	41.79(5)	39.18(8)	41.15(9){40.6}	42.66(15)–43.86(14)	41.1
τ[i]	-	5.37(17)	3.53(14)	0.50(39)–1.33(37)	-

[a] Data taken from ref. [11a]. [b] Data taken from ref. [11b]. [c] Data in brackets for **6** crystallized in triclinic unit cell taken from ref.[11b]. [d] Minimum and maximum data for the four non-equivalent molecules in the unit cell. [e] Cg(1) and Cg(2) are centroids of the C(1–5) and C(11–15) cyclopentadienyl rings, respectively. [f] Pl(1) and Pl(2) are least-squares planes of the C(1–5) and C(11–15) cyclopentadienyl rings, respectively. [g] C(a) and C(b) are acetylenic sp carbon atoms bearing substituents E for **4**: E(a) Me, E(b) Ph, for **6**: E(a) Ph, E(b) $SiMe_3$, for **7**: E(a) *t*-Bu, E(b) $SiMe_3$. [h] Dihedral angle between the least-squares planes of cyclopentadienyl rings. [i] Dihedral angle between the plane defined by Ti and C≡C atoms and the least-squares plane of the C≡C atoms and adjacent C or Si atoms.

Table 4 Bond lengths (Å) and bond angles (deg) for **11**

Bond lengths (Å)			
Ti–Cg(1)[a]	2.0868(10)	Ti–Cg(2)[a]	2.0809(10)
Ti–Pl(1)[b]	2.0854(3)	Ti–Pl(2)[b]	2.0809(3)
Ti–C(21)	2.177(3)	C(21)–C(22)	1.457(3)
Ti–C(22)	2.100(2)	C(22)–C(23)	1.304(3)
C(23)–C(24)	1.527(3)	C(24)–C(25)	1.517(3)
C(24)–C(26)	1.532(4)	C(24)–C(27)	1.526(3)
C(21)–H(21A)	1.04(3)	C(21)–H(21B)	1.03(3)
C(23)–H(23)	1.04(3)		
Bond angles (°)			
Cg(1)–Ti–Cg(2)[a]	144.56(4)	C(21)–Ti–C(22)	39.79(9)
Ti–C(21)–C(22)	67.25(13)	Ti–C(22)–C(21)	72.96(14)
C(21)–C(22)–C(23)	139.3(2)	C(22)–C(23)–C(24)	131.1(2)
C(23)–C(24)–C(25)	119.85(19)	C(22)–C(23)–H(23)	112.7(14)
C(24)–C(23)–H(23)	117.1(14)	H(21A)–C(21)–H(21B)	108.6(19)
Dihedral angles (°)			
φ[c]	37.58(8)	ψ(1)[d]	18.66(12)
ψ(2)[e]	19.17(13)		

[a] Cg(1) and Cg(2) are centroids of the C(1–5) and C(11–15) cyclopentadienyl rings, respectively. [b] Pl(1) and Pl(2) are least-squares planes of the C(1–5) and C(11–15) cyclopentadienyl rings, respectively. [c] Dihedral angle between Pl(1) and Pl(2). [d] Dihedral angle between Pl(1) and the Ti, C(21), and C(22) plane. [e] Dihedral angle between Pl(2) and the Ti, C(21), and C(22) plane.

Table 5 Electronic absorption spectra λ_{max} (nm), time dependent DFT excitation energies (nm) (in parentheses eV), Counterpoise Energy between the bent Cp^*_2Ti and the coordinated ethene or alkyne (kJ.mol^{-1}), Mayer bond orders, optimised bond lengths (Å), NBO atom charges q (e), and differences in atom charges for Ti and coordinated carbon atoms Δq (e) for **1**, and **3–9**

Cpd	Coordinated ligand	Electronic absorption spectrum[a]	Excitation energies (eV)	Counterpoise energy	Mayer BO Ti–C; C–C	*d* (calc.) Ti–C; C–C	*q*(NBO) (e)[b] Ti; C; C	Δq (e)[c]
1	CH_2=CH_2	940 <<< 360(sh)	909.48 (1.36) 411.11 (3.01) 388.45 (3.19)	−277.81	0.96; 1.37	2.141; 1.464	1.272; −0.650; −0.650	1.922
9	MeC≡CMe	660<<<340(sh)	632.93 (1.96) 539.28 (2.30) 376.60 (3.29)	−388.46	0.72; 1.69	2.038;1.314	1.278; −0.242; −0.238	1.518
3	PhC≡CPh	710 < 560 <<< 405 < 350	696.87 (1.78) 552.24 (2.25) 401.94 (3.08)	−390.21	0.68; 1.61	2.061; 1.318	1.303; −0.230; −0.238	1.537
4	PhC≡CMe	705 ~ 555 << 405(sh) <330	643.03 (1.93) 559.63 (2.22) 382.84 (3.24)	−388.97	0.72; 1.74	2.052; 1.316	1.292; −0.281; −0.187	1.526
5	Me_3SiC≡CMe	775 > 515 <<< 390	722.72 (1.72) 504.49 (2.46) 374.31 (3.31)	−359.48	0.71; 1.75	2.058; 1.318	1.310; −0.767; −0.178	1.783
6	Me_3SiC≡CPh	780 > 535 <<<410(sh) < 370(sh) < 327(sh)	739.09 (1.68) 529.96 (2.34) 409.99 (3.02)	−361.35	0.70; 1.72	2.070; 1.321	1.317; −0.722; −0.217	1.787
7	Me_3SiC≡$CCMe_3$	850 > 530 <<< 402	791.49 (1.57)	−360.74	0.72; 1.76	2.080; 1.320	1.376; −0.766; −0.201	1.860

		< 330(sh)	523.18 (2.40) 391.29 (3.17)					
8	$Me_3SiC{\equiv}CSiMe_3$	920[a] > 505(sh) <<< 390	847.97 (1.46) 491.26 (2.52) 406.81 (3.05)	−330.40	0.69; 1.74	2.083; 1.324	1.327; −0.709; −0.705	2.034

[a] Experimental spectra (reproduced in ESI) are described by relative band absorbances except for **8**: molar extinction coefficient at λ_{max} 920 nm ε = 81(3) $cm^2.mmol^{-1}$.

[b] The order of acetylenic carbon atoms is as given in alkyne formulae.

[c] Δq is the difference between the charge on titanium atom and the average charge on the ligand carbon atoms (q(Ti) $-q_{av}$(C)).

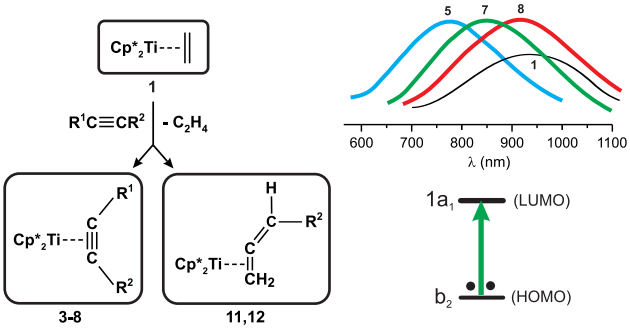
Cp*2Ti---
1
R1C≡CR2
- C2H4
R1
C
Cp*2Ti---
C
R2
3-8
H
C
R2
C
Cp*2Ti---
CH2
11,12
5
7
8
1
600
700
800
900
1000
1100
λ (nm)
1a1
(LUMO)
b2
(HOMO)

Internal alkyne substituents control the first excitation energy of decamethyltitanocene-η^2-alkyne complexes and isomerisation to η^2-allene complexes.